Advanced Soil Mechanics

Braja M. Das

CRC Press
Taylor & Francis Group

Advanced Soil Mechanics

Fifth Edition

Taylor & Francis
Taylor & Francis Group
http://taylorandfrancis.com

Advanced Soil Mechanics

Fifth Edition

Braja M. Das

CRC Press
Taylor & Francis Group
Boca Raton London New York

CRC Press is an imprint of the
Taylor & Francis Group, an **informa** business

CRC Press
Taylor & Francis Group
6000 Broken Sound Parkway NW, Suite 300
Boca Raton, FL 33487-2742

CRC Press is an imprint of Taylor & Francis Group, an Informa business

No claim to original U.S. Government works

Printed on acid-free paper

International Standard Book Number-13: 978-0-8153-7913-3 (Hardback)

Library of Congress Cataloging-in-Publication Data

Names: Das, Braja M., 1941- author.
Title: Advanced soil mechanics / Braja Das.
Description: 5th edition. | Boca Raton : Taylor & Francis, a CRC title, part of the Taylor & Francis imprint, a member of the Taylor & Francis Group, the academic division of T&F Informa, plc, [2019] | Includes bibliographical references and index. |
Identifiers: LCCN 2018047522 (print) | LCCN 2018047957 (ebook) | ISBN 9781351215169 (ePub) | ISBN 9781351215152 (Mobipocket) | ISBN 9781351215176 (Adobe PDF) | ISBN 9780815379133 (hardback) | ISBN 9781351215183 (ebook)
Subjects: LCSH: Soil mechanics--Textbooks.
Classification: LCC TA710 (ebook) | LCC TA710 .D257 2019 (print) | DDC 624.1/5136--dc23
LC record available at https://lccn.loc.gov/2018047522

Visit the Taylor & Francis Web site at
http://www.taylorandfrancis.com

and the CRC Press Web site at
http://www.crcpress.com

To
Janice, Joe, Valerie, and Elizabeth

Taylor & Francis
Taylor & Francis Group
http://taylorandfrancis.com

Contents

Preface

This textbook is intended for use in an introductory graduate level course that broadens (expands) the fundamental concepts acquired by students in their undergraduate work. The introductory graduate course can be followed by advanced courses dedicated to topics such as mechanical and chemical stabilization of soils, geoenvironmental engineering, finite element application to geotechnical engineering, critical state soil mechanics, geosynthetics, rock mechanics, and others.

The first edition of this book was published jointly by Hemisphere Publishing Corporation and McGraw-Hill Book Company of New York with a 1983 copyright. Taylor & Francis Group published the second, third, and fourth editions with 1997, 2008, and 2014 copyrights, respectively. The book has a total of 11 chapters and an appendix. SI units have been used throughout the text.

The following is a summary of additional materials given in this edition.

- Several new example problems have been added. The book now has more than 100 example problems which help the readers understand the theories presented. About 70 additional line drawings have been added to the text.
- In Chapter 1, "Soil aggregate, plasticity, and classification," relationships for determination of liquid limit by one-point method from test results of fall cone have been added to Section 1.8.1. Section 1.13.1 provides several correlations for estimation of the relative density of granular soil. This section also has correlations between uniformity coefficient, angularity, and maximum and minimum void ratios of granular soil. Effect of nonplastic fines on maximum and minimum void ratios of granular soils is given in Section 1.14.1.
- In Chapter 3, "Stresses and displacements in a soil mass—two-dimensional problems," stress determination for vertical line load located at the apex of an infinite wedge is presented in Section 3.3. Section 3.7 provides stress relationships for horizontal and inclined line loads

acting at the apex of an infinite wedge. Section 3.12 describes the stress distribution under a symmetrical vertical triangular strip load.

- In Chapter 4, "Stresses and displacements in a soil mass—three-dimensional problems," vertical stress calculation below flexible circular area with parabolic and conical loading are presented in Sections 4.10 and 4.11, respectively. Also a relationship for vertical stress under a uniformly loaded flexible elliptical area is given in Section 4.12.
- In Chapter 8, "Consolidation," Section 8.1 explains the fundamentals of the time-dependent settlement of saturated cohesive soil using the behavior of Kelvin model under load. Section 8.3.1 provides a simplified procedure developed by Hanna et al. (2013) to estimate the average degree of consolidation due to ramp loading. The log-log method proposed by Jose et al. (1989) and the Oikawa method (1987) to determine the preconsolidation pressure have been discussed in Section 8.5.1.1. A compilation of several correlations presently available in the literature for the recompression index of clay is given in Table 8.5. Design curves for prefabricated vertical drains have been elaborated upon in Section 8.17.
- In Chapter 9, "Shear strength of soils," the relevance of various laboratory test methods to field conditions has been briefly discussed in Section 9.4. In Section 9.7 a discussion has been provided to quantify the difference between the secant friction angle (ϕ_{secant}) and the ultimate friction angle (ϕ_{cv}) of granular soils based on the analysis of Bolten (1968). This section also includes the correlations for ϕ_{cv} for single mineral soil as discussed by Koerner (1970). Recently developed correlations for drained friction angle of normally consolidated clay (Sorensen and Okkels, 2013) are summarized in Section 9.12. Section 9.15 provides several correlations for the undrained shear strength of remolded clay. Relationships for determination of undrained shear strength using tapered vanes have been added to Section 9.22.
- In Chapter 10, "Elastic settlement of shallow foundations," the strain influence factor method for settlement calculation as provided by Terzaghi et al. (1996) has been discussed in Section 10.5.2. Settlement calculation based on the theory of elasticity as given in Section 10.6.1 has been substantially expanded. Elastic settlement in granular soil considering the change in soil modulus with elastic strain, and the effect of ground water table rise on elastic settlement of shallow foundations on granular soil have been discussed in two new sections: Sections 10.7 and 10.8.
- In Chapter 11, "Consolidation settlement of shallow foundations," discussion of Griffith's (1984) influence factor for determination of the average vertical stress increase in a soil layer has been added to Section 11.2.

Acknowledgments

Thanks are due to my wife, Janice, for her help in preparing the revised manuscript. I would also like to thank Tony Moore, senior editor, and Gabriella Williams, editorial assistant, Taylor & Francis Group, for working with me during the entire publication process of the book.

Thanks are due to Professor Nagaratnam Sivakugan of the College of Science, Technology, and Engineering, James Cook University, Queensland, Australia, for providing the cover page image.

Braja M. Das

Taylor & Francis
Taylor & Francis Group
http://taylorandfrancis.com

Author

Braja M. Das is the Dean Emeritus of the College of Engineering and Computer Science at California State University, USA. He is a Fellow and Life Member of the American Society of Civil Engineers, a Life Member of the American Society for Engineering Education, and an Emeritus Member of the Transportation Research Board (TRB) AFS-80 Committee on Stabilization of Geomaterials and Stabilized Materials.

Professor Das is the author or coauthor of several textbooks and reference books in the area of geotechnical engineering, and he is Founder and Editor-in-Chief of the *International Journal of Geotechnical Engineering*.

Taylor & Francis
Taylor & Francis Group
http://taylorandfrancis.com

Chapter 1

Soil aggregate, plasticity, and classification

1.1 INTRODUCTION

Soils are aggregates of mineral particles; and together with air and/or water in the void spaces, they form three-phase systems. A large portion of the earth's surface is covered by soils, and they are widely used as construction and foundation materials. Soil mechanics is the branch of engineering that deals with the engineering properties of soils and their behavior under stress.

This book is divided into 11 chapters: "Soil Aggregate, Plasticity, and Classification," "Stresses and Strains: Elastic Equilibrium," "Stresses and Displacement in a Soil Mass: Two-Dimensional Problems," "Stresses and Displacement in a Soil Mass: Three-Dimensional Problems," "Pore Water Pressure due to Undrained Loading," "Permeability," "Seepage," "Consolidation," "Shear Strength of Soil," "Elastic Settlement of Shallow Foundations," and "Consolidation Settlement of Shallow Foundations." This chapter is a brief overview of some soil properties and their classification. It is assumed that the reader has been previously exposed to a basic soil mechanics course.

1.2 SOIL: SEPARATE SIZE LIMITS

A naturally occurring soil sample may have particles of various sizes. Over the years, various agencies have tried to develop the size limits of gravel, sand, silt, and clay. Some of these size limits are shown in Table 1.1.

Referring to Table 1.1, it is important to note that some agencies classify clay as particles smaller than 0.005 mm in size, and others classify it as particles smaller than 0.002 mm in size. However, it needs to be realized that particles defined as clay on the basis of their size are not necessarily clay minerals. Clay particles possess the tendency to develop plasticity when mixed with water; these are clay minerals. Kaolinite, illite, montmorillonite, vermiculite, and chlorite are examples of some clay minerals.

Table 1.1 Soil: separate size limits

Agency	*Classification*	*Size limits (mm)*
U.S. Department of Agriculture (USDA)	Gravel	>2
	Very coarse sand	2–1
	Coarse sand	1–0.5
	Medium sand	0.5–0.25
	Fine sand	0.25–0.1
	Very fine sand	0.1–0.05
	Silt	0.05–0.002
	Clay	<0.002
International Society of Soil Mechanics and Geotechnical Engineering (ISSMGE)	Gravel	>2
	Coarse sand	2–0.2
	Fine sand	0.2–0.02
	Silt	0.02–0.002
	Clay	<0.002
Federal Aviation Administration (FAA)	Gravel	>2
	Sand	2–0.075
	Silt	0.075–0.005
	Clay	<0.005
Massachusetts Institute of Technology (MIT)	Gravel	>2
	Coarse sand	2–0.6
	Medium sand	0.6–0.2
	Fine sand	0.2–0.06
	Silt	0.06–0.002
	Clay	<0.002
American Association of State Highway and Transportation Officials (AASHTO)	Gravel	76.2–2
	Coarse sand	2–0.425
	Fine sand	0.425–0.075
	Silt	0.075–0.002
	Clay	<0.002
Unified (U.S. Army Corps of Engineers, U.S. Bureau of Reclamation, and American Society for Testing and Materials)	Gravel	76.2–4.75
	Coarse sand	4.75–2
	Medium sand	2–0.425
	Fine sand	0.425–0.075
	Silt and clay (fines)	<0.075

Fine particles of quartz, feldspar, or mica may be present in a soil in the size range defined for clay, but these will not develop plasticity when mixed with water. It appears that it is more appropriate for soil particles with sizes <2 or 5 μm as defined under various systems to be called *clay-size particles* rather than *clay*. True clay particles are mostly of colloidal size range (<1 μm), and 2 μm is probably the upper limit.

1.3 CLAY MINERALS

Clay minerals are complex silicates of aluminum, magnesium, and iron. Two basic crystalline units form the clay minerals: (1) a silicon–oxygen tetrahedron, and (2) an aluminum or magnesium octahedron. A silicon–oxygen tetrahedron unit, shown in Figure 1.1a, consists of four oxygen atoms surrounding a silicon atom. The tetrahedron units combine to form a *silica sheet* as shown in Figure 1.2a. Note that the three oxygen atoms located at the base of each tetrahedron are shared by neighboring tetrahedra. Each silicon atom with a positive valence of 4 is linked to four oxygen atoms with a total negative valence of 8. However, each oxygen atom at the base of the tetrahedron is linked to two silicon atoms. This leaves one negative valence charge of the top oxygen atom of each tetrahedron to be counterbalanced. Figure 1.1b shows an octahedral unit consisting of six hydroxyl units surrounding an aluminum (or a magnesium) atom. The combination of the aluminum octahedral units forms a *gibbsite sheet* (Figure 1.2b). If the main metallic atoms in the octahedral units are magnesium, these sheets are referred to as *brucite sheets*. When the silica sheets are stacked over the octahedral sheets, the oxygen atoms replace the hydroxyls to satisfy their valence bonds. This is shown in Figure 1.2c.

Some clay minerals consist of repeating layers of two-layer sheets. A two-layer sheet is a combination of a silica sheet with a gibbsite sheet, or a combination of a silica sheet with a brucite sheet. The sheets are about 7.2 Å thick. The repeating layers are held together by hydrogen bonding and secondary valence forces. *Kaolinite* is the most important clay mineral belonging to this type (Figure 1.3). Figure 1.4 shows a scanning electron micrograph of kaolinite. Other common clay minerals that fall into this category are *serpentine* and *halloysite*.

The most common clay minerals with three-layer sheets are *illite* and *montmorillonite* (Figure 1.5). A three-layer sheet consists of an octahedral sheet in the middle with one silica sheet at the top and one at the bottom. Repeated layers of these sheets form the clay minerals. *Illite* layers

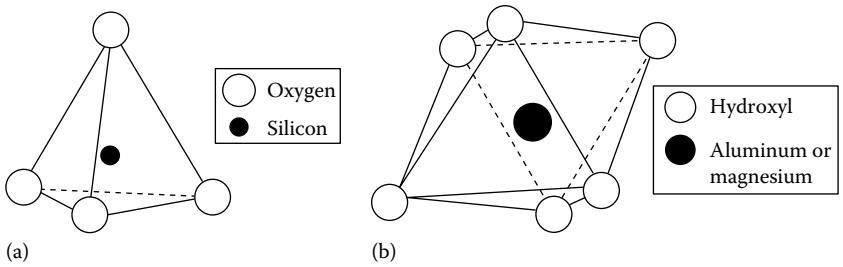

Figure 1.1 (a) Silicon–oxygen tetrahedron unit and (b) aluminum or magnesium octahedral unit.

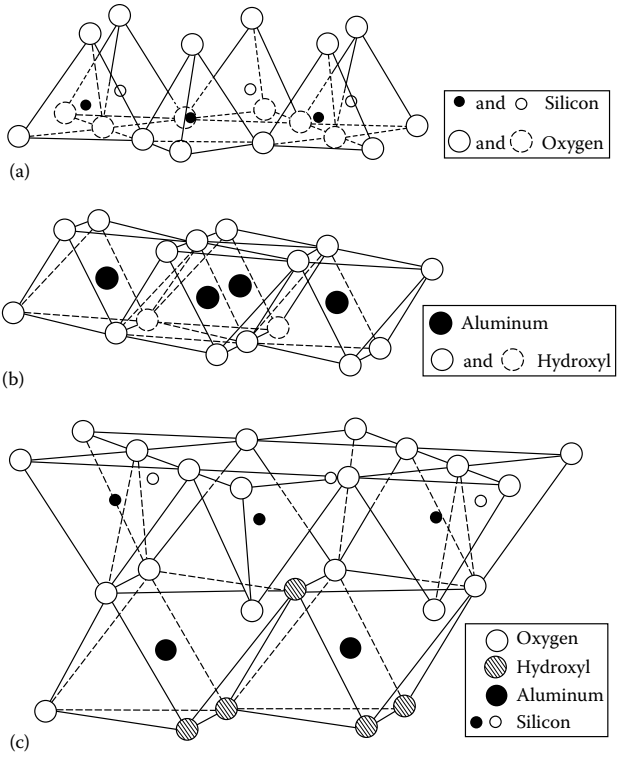

Figure 1.2 (a) Silica sheet, (b) gibbsite sheet, and (c) silica–gibbsite sheet. [After Grim, R. E., *J. Soil Mech. Found. Div.,* ASCE, 85(2), 1–17, 1959.]

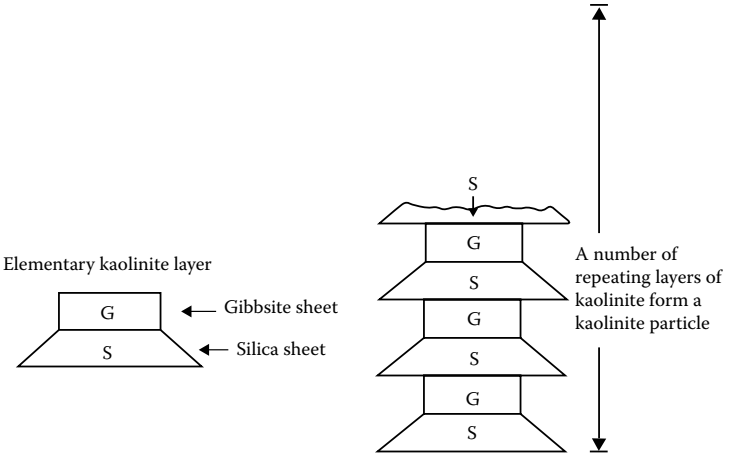

Figure 1.3 Symbolic structure for kaolinite.

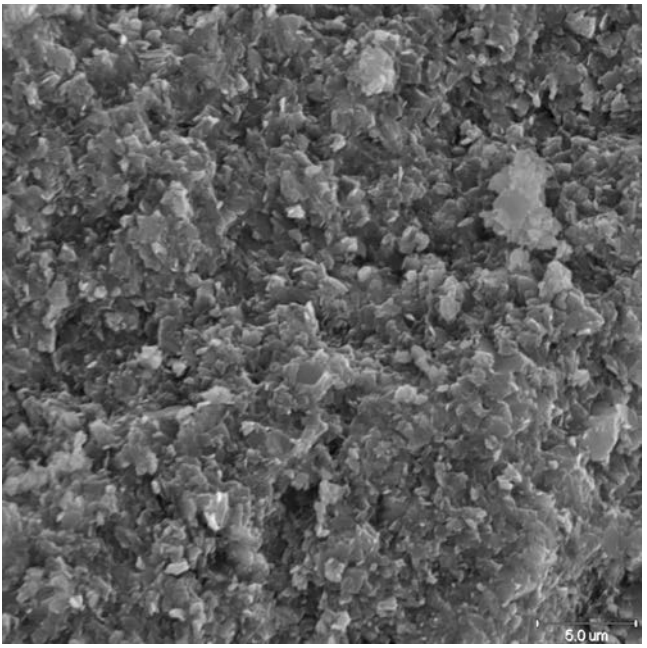

Figure 1.4 Scanning electron micrograph of a kaolinite specimen. (Courtesy of David J. White, Ingios Geotechnics, Inc. Northfield, Minnesota.)

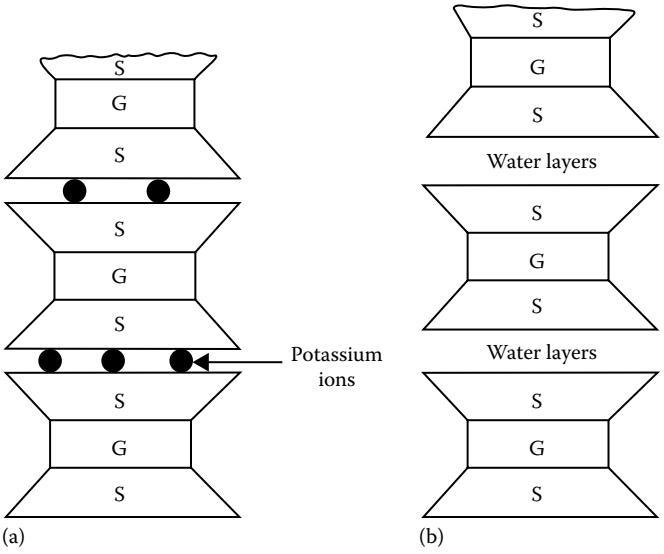

Figure 1.5 Symbolic structure of (a) illite and (b) montmorillonite.

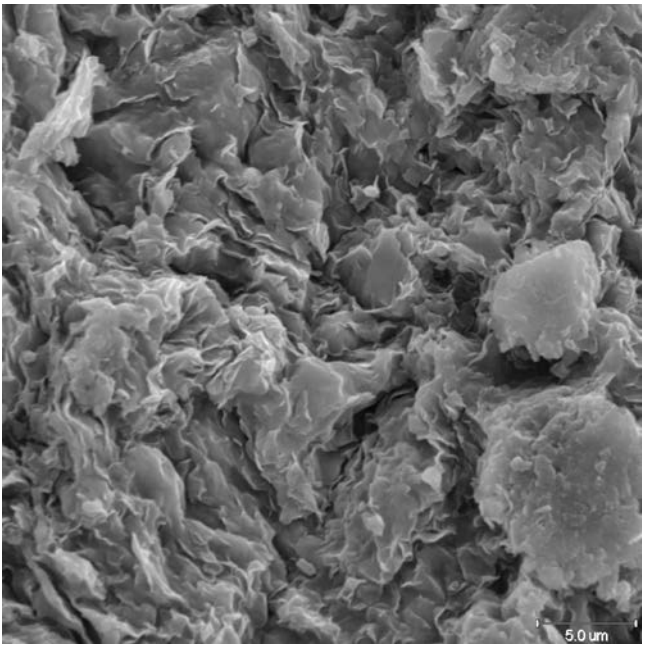

Figure 1.6 Scanning electron micrograph of a montmorillonite specimen. (Courtesy of David J, White, Ingios Geotechnics, Inc. Northfield, Minnesota.)

are bonded together by potassium ions. The negative charge to balance the potassium ions comes from the substitution of aluminum for some silicon in the tetrahedral sheets. Substitution of this type by one element for another without changing the crystalline form is known as *isomorphous substitution*. *Montmorillonite* has a similar structure to illite. However, unlike illite, there are no potassium ions present, and a large amount of water is attracted into the space between the three-sheet layers. Figure 1.6 shows a scanning electron micrograph of montmorillonite.

The surface area of clay particles per unit mass is generally referred to as *specific surface*. The lateral dimensions of kaolinite platelets are about 1,000–20,000 Å with thicknesses of 100–1,000 Å. Illite particles have lateral dimensions of 1000–5000 Å and thicknesses of 50–500 Å. Similarly, montmorillonite particles have lateral dimensions of 1000–5000 Å with thicknesses of 10–50 Å. If we consider several clay samples all having the same mass, the highest surface area will be in the sample in which the particle sizes are the smallest. So it is easy to realize that the specific surface of kaolinite will be small compared to that of montmorillonite. The specific surfaces of kaolinite, illite, and montmorillonite are about 15, 90, and 800 m^2/g, respectively. Table 1.2 lists the specific surfaces of some clay minerals.

Table 1.2 Specific surface area and cation exchange capacity of some clay minerals

Clay mineral	*Specific surface (m^2/g)*	*Cation exchange capacity (me/100 g)*
Kaolinite	10–20	3
Illite	80–100	25
Montmorillonite	800	100
Chlorite	5–50	20
Vermiculite	5–400	150
Halloysite ($4H_2O$)	40	12
Halloysite ($2H_2O$)	40	12

Clay particles carry a net negative charge. In an ideal crystal, the positive and negative charges would be balanced. However, isomorphous substitution and broken continuity of structures result in a net negative charge at the faces of the clay particles. (There are also some positive charges at the edges of these particles.) To balance the negative charge, the clay particles attract positively charged ions from salts in their pore water. These are referred to as exchangeable ions. Some are more strongly attracted than others, and the cations can be arranged in a series in terms of their affinity for attraction as follows:

$$Al^{3+} > Ca^{2+} > Mg^{2+} > NH_4^+ > K^+ > H^+ > Na^+ > Li^+$$

This series indicates that, for example, Al^{3+} ions can replace Ca^{2+} ions, and Ca^{2+} ions can replace Na^+ ions. The process is called *cation exchange*. For example,

$$Na_{clay} + CaCl_2 \rightarrow Ca_{clay} + NaCl$$

Cation exchange capacity (CEC) of a clay is defined as the amount of exchangeable ions, expressed in milliequivalents, per 100 g of dry clay. Table 1.2 gives the CEC of some clays.

1.4 NATURE OF WATER IN CLAY

The presence of exchangeable cations on the surface of clay particles was discussed in the preceding section. Some salt precipitates (cations in excess of the exchangeable ions and their associated anions) are also present on the surface of dry clay particles. When water is added to clay, these cations and anions float around the clay particles (Figure 1.7).

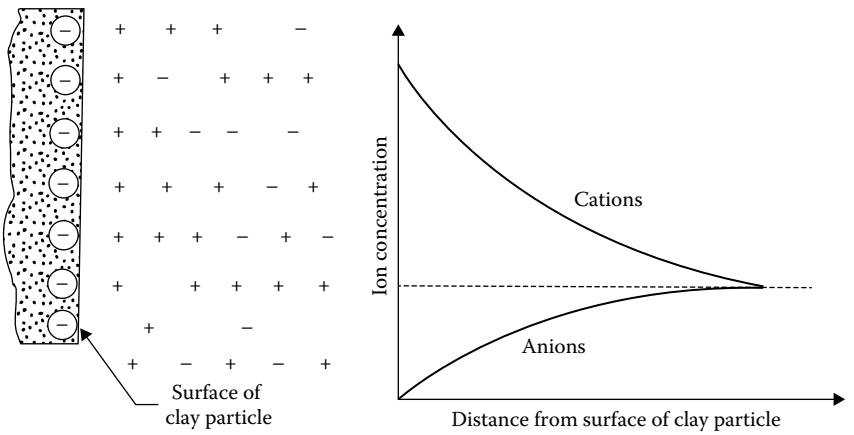

Figure 1.7 Diffuse double layer.

At this point, it must be pointed out that water molecules are dipolar, since the hydrogen atoms are not symmetrically arranged around the oxygen atoms (Figure 1.8a). This means that a molecule of water is like a rod with positive and negative charges at opposite ends (Figure 1.8b). There are three general mechanisms by which these dipolar water molecules, or *dipoles*, can be electrically attracted toward the surface of the clay particles (Figure 1.9):

a. Attraction between the negatively charged faces of clay particles and the positive ends of dipoles
b. Attraction between cations in the double layer and the negatively charged ends of dipoles. The cations are in turn attracted by the negatively charged faces of clay particles
c. Sharing of the hydrogen atoms in the water molecules by hydrogen bonding between the oxygen atoms in the clay particles and the oxygen atoms in the water molecules

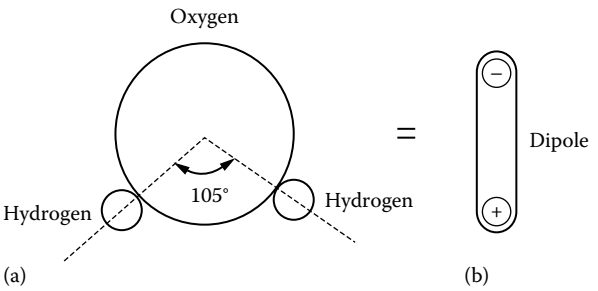

Figure 1.8 Dipolar nature of water: (a) unsymmetrical arrangement of hydrogen atoms; (b) dipole.

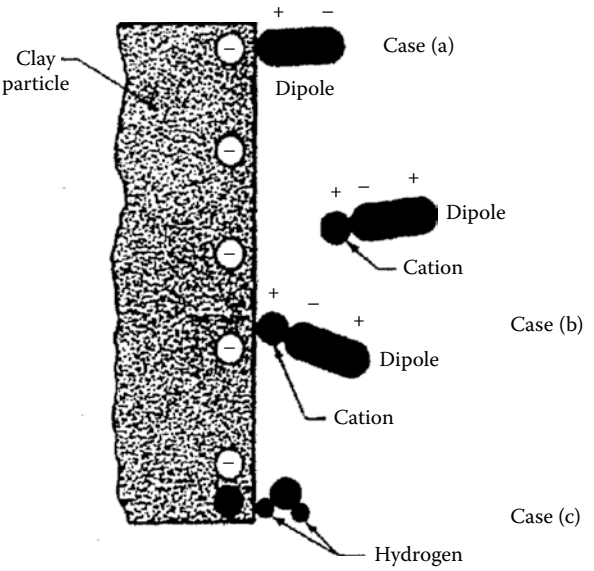

Figure 1.9 Dipolar water molecules in diffuse double layer.

The electrically attracted water that surrounds the clay particles is known as *double-layer water*. The plastic property of clayey soils is due to the existence of double-layer water. Thicknesses of double-layer water for typical kaolinite and montmorillonite crystals are shown in Figure 1.10. Since the innermost layer of double-layer water is very strongly held by a clay particle, it is referred to as *adsorbed water*.

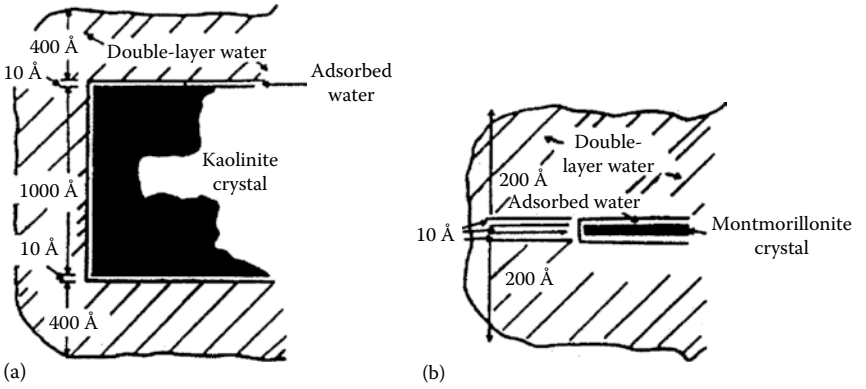

Figure 1.10 Clay water (a) typical kaolinite particle, 10,000 by 1,000 Å and (b) typical montmorillonite particle, 1,000 by 10 Å. [After Lambe, T. W., *Trans.* ASCE, 125, 682, 1960.]

1.5 REPULSIVE POTENTIAL

The nature of the distribution of ions in the diffuse double layer is shown in Figure 1.7. Several theories have been presented in the past to describe the ion distribution close to a charged surface. Of these, the Gouy–Chapman theory has received the most attention. Let us assume that the ions in the double layers can be treated as point charges, and that the surface of the clay particles is large compared to the thickness of the double layer. According to Boltzmann's theorem, we can write that (Figure 1.11)

$$n_+ = n_{+(0)} \exp \frac{-v_+ e\Phi}{KT} \tag{1.1}$$

$$n_- = n_{-(0)} \exp \frac{-v_- e\Phi}{KT} \tag{1.2}$$

where

n_+ is the local concentration of positive ions at a distance x
n_- is the local concentration of negative ions at a distance x
$n_{+(0)}$, $n_{-(0)}$ are the concentration of positive and negative ions away from the clay surface in the equilibrium liquid
Φ is the average electric potential at a distance x (Figure 1.12)
v_+, v_- are ionic valences
e is the unit electrostatic charge, 4.8×10^{-10} esu
K is the Boltzmann constant, 1.38×10^{-16} erg/K
T is the absolute temperature

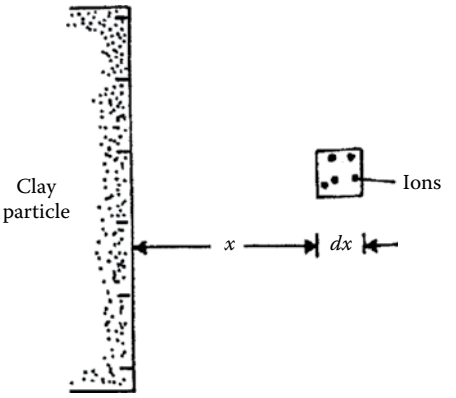

Figure 1.11 Derivation of repulsive potential equation.

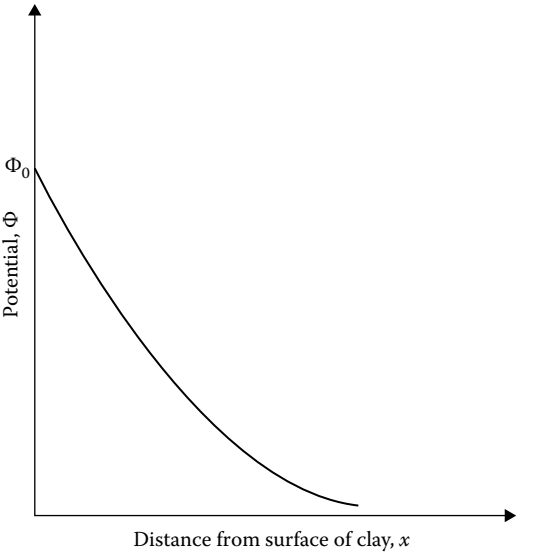

Figure 1.12 Nature of variation of potential Φ with distance from the clay surface.

The charge density ρ at a distance x is given by

$$\rho = \nu_+ en_+ - \nu_- en_- \tag{1.3}$$

According to Poisson's equation

$$\frac{d^2\Phi}{dx^2} = \frac{-4\pi\rho}{\lambda} \tag{1.4}$$

where λ is the dielectric constant of the medium.

Assuming $\nu_+ = \nu_-$ and $n_{+(0)} = n_{-(0)} = n_0$, and combining Equations 1.1 through 1.4, we obtain

$$\frac{d^2\Phi}{dx^2} = \frac{8\pi n_0 \nu e}{\lambda} \sinh \frac{\nu e \Phi}{KT} \tag{1.5}$$

It is convenient to rewrite Equation 1.5 in terms of the following nondimensional quantities

$$y = \frac{\nu e \Phi}{KT} \tag{1.6}$$

$$z = \frac{\nu e \Phi_0}{KT} \tag{1.7}$$

and

$$\xi = \kappa x \tag{1.8}$$

where Φ_0 is the potential at the surface of the clay particle and

$$\kappa^2 = \frac{8\pi n_0 e^2 v^2}{\lambda KT} (\text{cm}^{-2}) \tag{1.9}$$

Thus, from Equation 1.5

$$\frac{d^2y}{d\xi^2} = \sinh y \tag{1.10}$$

The boundary conditions for solving Equation 1.10 are

1. At $\xi = \infty$, $y = 0$ and $dy/d\xi = 0$
2. At $\xi = 0$, $y = z$, that is, $\Phi = \Phi_0$

The solution yields the relation

$$e^{y/2} = \frac{(e^{z/2}+1)+(e^{z/2}-1)e^{-\xi}}{(e^{z/2}+1)-(e^{z/2}-1)e^{-\xi}} \tag{1.11}$$

Equation 1.11 gives an approximately exponential decay of potential. The nature of the variation of the nondimensional potential y with the nondimensional distance is given in Figure 1.13.

For a small surface potential (<25 mV), we can approximate Equation 1.5 as

$$\frac{d^2\Phi}{dx^2} = \kappa^2\Phi \tag{1.12}$$

$$\Phi = \Phi_0 e^{-\kappa x} \tag{1.13}$$

Equation 1.13 describes a purely exponential decay of potential. For this condition, the center of gravity of the diffuse charge is located at a distance of $x = 1/\kappa$. The term $1/\kappa$ is generally referred to as the double-layer *thickness*.

There are several factors that will affect the variation of the repulsive potential with distance from the surface of the clay layer. The effect of the cation concentration and ionic valence is shown in Figures 1.14 and 1.15, respectively. For a given value of Φ_0 and x, the repulsive potential Φ decreases with the increase of ion concentration n_0 and ionic valence v.

When clay particles are close and parallel to each other, the nature of variation of the potential will be as shown in Figure 1.16. Note for this case

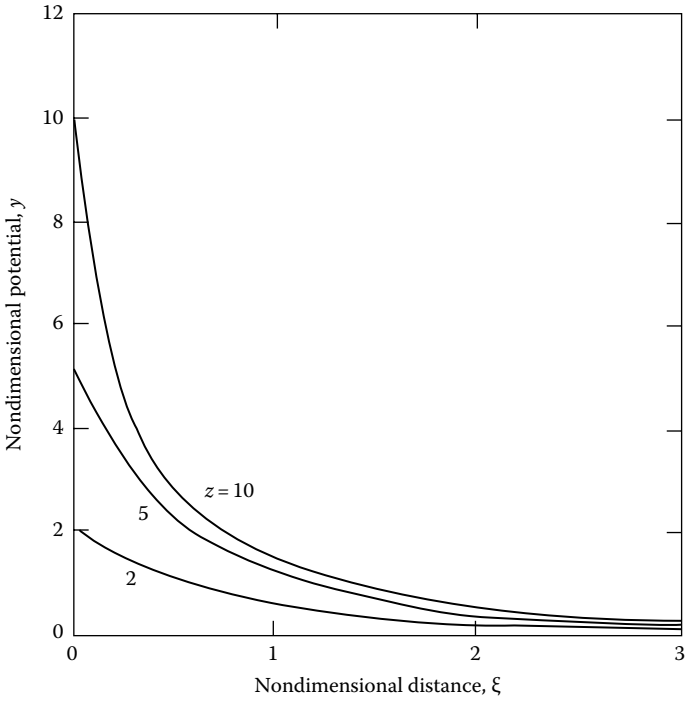

Figure 1.13 Variation of nondimensional potential with nondimensional distance.

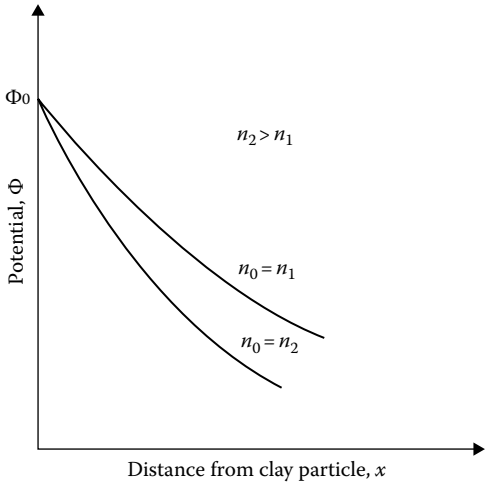

Figure 1.14 Effect of cation concentration on the repulsive potential.

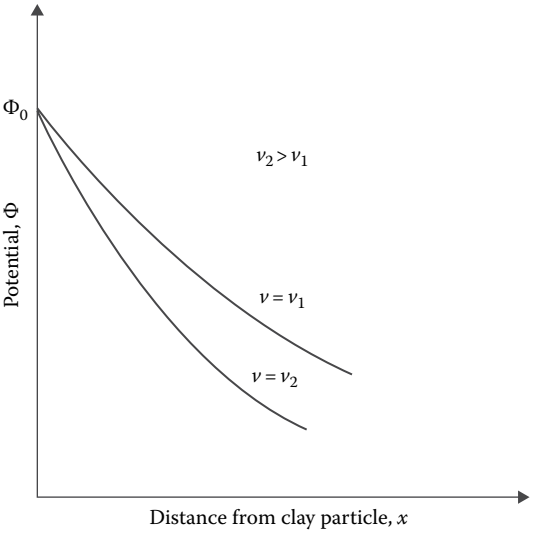

Figure 1.15 Effect of ionic valence on the repulsive potential.

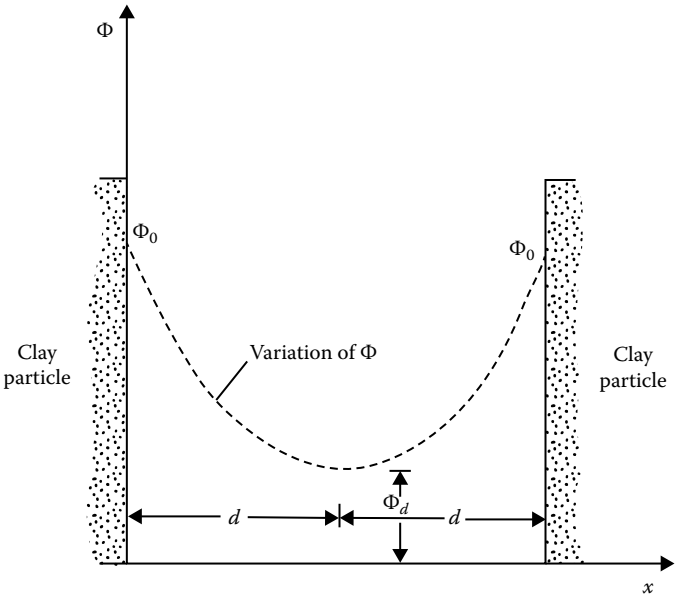

Figure 1.16 Variation of Φ between two parallel clay particles.

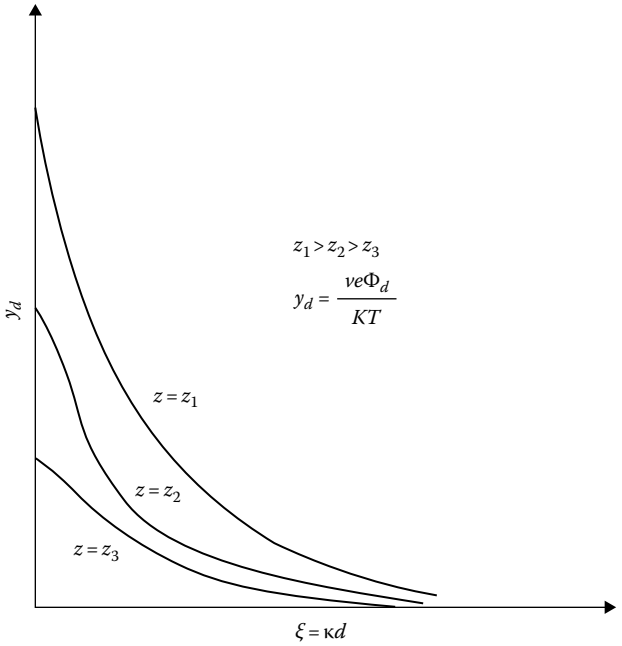

Figure 1.17 Nature of variation of the nondimensional midplane potential for two parallel plates.

that at $x = 0$, $\Phi = \Phi_0$, and at $x = d$ (midway between the plates), $\Phi = \Phi_d$ and $d\Phi/dx = 0$. Numerical solutions for the nondimensional potential $y = y_d$ (i.e., $\Phi = \Phi_d$) for various values of z and $\xi = \kappa d$ (i.e., $x = d$) are given by Verweg and Overbeek (1948) (see also Figure 1.17).

1.6 REPULSIVE PRESSURE

The repulsive pressure midway between two parallel clay plates (Figure 1.18) can be given by the Langmuir equation

$$p = 2n_0 KT\left(\cosh\frac{ve\Phi_d}{KT} - 1\right) \tag{1.14}$$

where p is the repulsive pressure, that is, the difference between the osmotic pressure midway between the plates in relation to that in the equilibrium solution. Figure 1.19, which is based on the results of Bolt (1956), shows the theoretical and experimental variation of p between two clay particles.

Although the Guoy–Chapman theory has been widely used to explain the behavior of clay, there have been several important objections to this theory. A good review of these objections has been given by Bolt (1955).

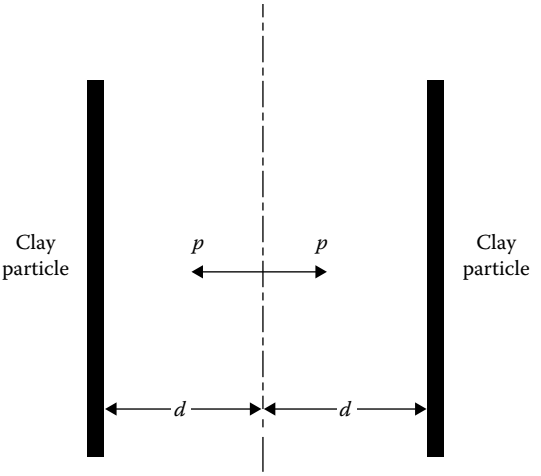

Figure 1.18 Repulsive pressure midway between two parallel clay plates.

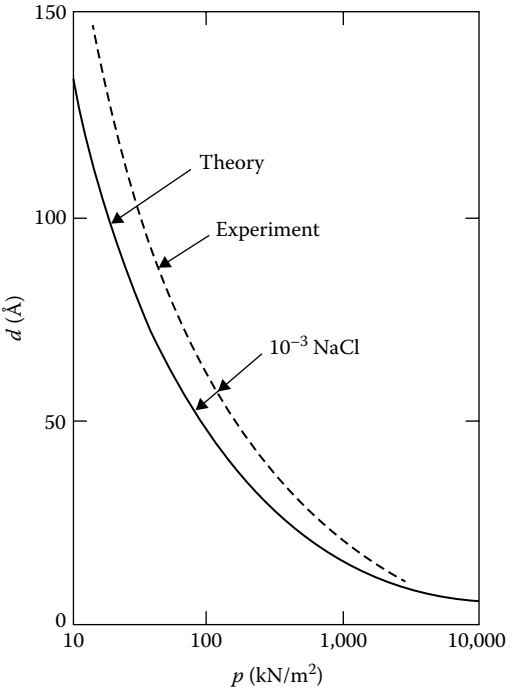

Figure 1.19 Repulsive pressure between sodium montmorillonite clay particles. [After Bolt, G. H., *Geotechnique*, 6(2), 86, 1956.]

1.7 FLOCCULATION AND DISPERSION OF CLAY PARTICLES

In addition to the repulsive force between the clay particles, there is an attractive force, which is largely attributed to the Van der Waal force. This is a secondary bonding force that acts between all adjacent pieces of matter. The force between two flat parallel surfaces varies inversely as $1/x^3$ to $1/x^4$, where x is the distance between the two surfaces. Van der Waal's force is also dependent on the dielectric constant of the medium separating the surfaces. However, if water is the separating medium, substantial changes in the magnitude of the force will not occur with minor changes in the constitution of water.

The behavior of clay particles in a suspension can be qualitatively visualized from our understanding of the attractive and repulsive forces between the particles and with the aid of Figure 1.20. Consider a dilute suspension of clay particles in water. These colloidal clay particles will undergo Brownian movement and, during this random movement, will come close to

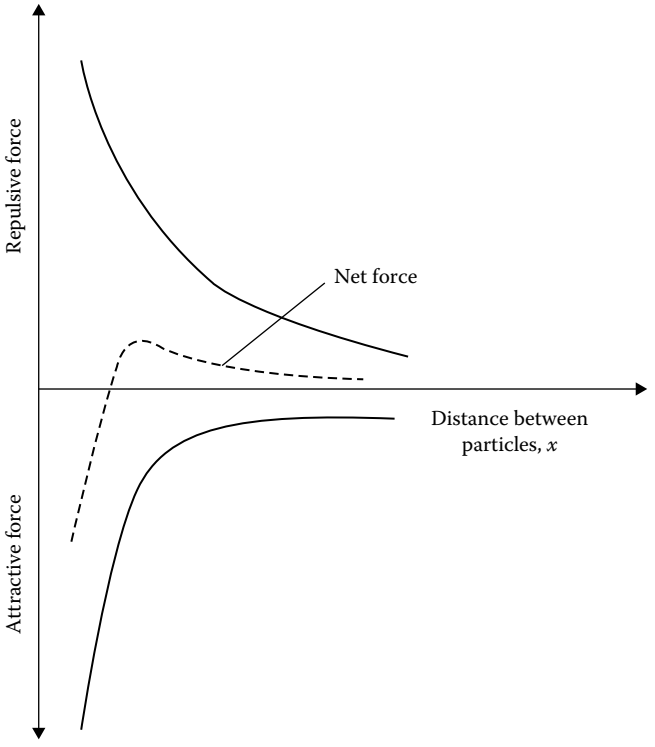

Figure 1.20 Dispersion and flocculation of clay in a suspension.

each other at distances within the range of interparticle forces. The forces of attraction and repulsion between the clay particles vary at different rates with respect to the distance of separation. The force of repulsion decreases exponentially with distance, whereas the force of attraction decreases as the inverse third or fourth power of distance, as shown in Figure 1.20. Depending on the distance of separation, if the magnitude of the repulsive force is greater than the magnitude of the attractive force, the net result will be repulsion. The clay particles will settle individually and form a dense layer at the bottom; however, they will remain separate from their neighbors (Figure 1.21a). This is referred to as the *dispersed state* of the soil. On the contrary, if the net force between the particles is attraction, flocs will be formed and these flocs will settle to the bottom. This is called *flocculated* clay (Figure 1.21b).

1.7.1 Salt flocculation and nonsalt flocculation

We saw in Figure 1.14 the effect of salt concentration, n_0, on the repulsive potential of clay particles. High salt concentration will depress the double layer of clay particles and hence the force of repulsion. We noted earlier in this section that the Van der Waal force largely contributes to the force of attraction between clay particles in suspension. If the clay particles are suspended in water with a high salt concentration, the flocs of the clay particles formed by dominant attractive forces will give them mostly an orientation approaching parallelism (face-to-face type). This is called a salt-type flocculation (Figure 1.22a).

Another type of force of attraction between the clay particles, which is not taken into account in colloidal theories, is that arising from the electrostatic attraction of the positive charges at the edge of the particles and the negative charges at the face. In a soil–water suspension with low salt concentration, this electrostatic force of attraction may produce a flocculation with an orientation approaching a perpendicular array. This is shown in Figure 1.22b and is referred to as nonsalt flocculation.

Figure 1.21 (a) Dispersion and (b) flocculation of clay.

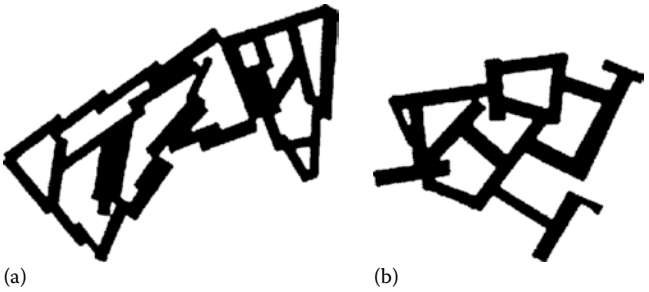

Figure 1.22 (a) Salt and (b) nonsalt flocculation of clay particles.

1.8 CONSISTENCY OF COHESIVE SOILS

The presence of clay minerals in a fine-grained soil will allow it to be remolded in the presence of some moisture without crumbling. If a clay slurry is dried, the moisture content will gradually decrease, and the slurry will pass from a liquid state to a plastic state. With further drying, it will change to a semisolid state and finally to a solid state, as shown in Figure 1.23. In 1911, A. Atterberg, a Swedish scientist, developed a method for describing the limit consistency of fine-grained soils on the basis of moisture content. These limits are the *liquid limit*, the *plastic limit*, and the *shrinkage limit*.

The liquid limit is defined as the moisture content, in percent, at which the soil changes from a liquid state to a plastic state. The moisture contents (in percent) at which the soil changes from a plastic to a semisolid state and from a semisolid to a solid state are defined as the plastic limit and the shrinkage limit, respectively. These limits are generally referred to as the *Atterberg limits*. The Atterberg limits of cohesive soil depend on several factors, such as the amount and type of clay minerals and the type of adsorbed cation.

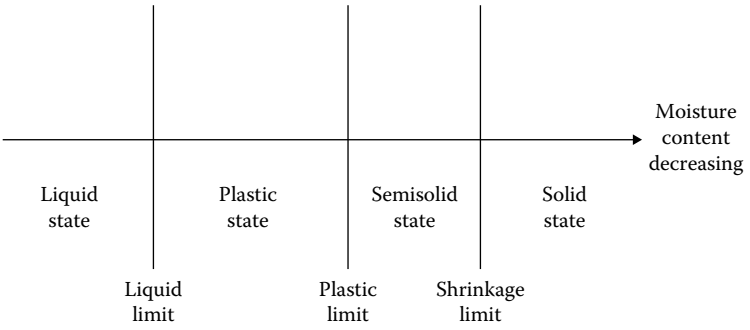

Figure 1.23 Consistency of cohesive soils.

1.8.1 Liquid limit

The liquid limit of a soil is generally determined by the Standard Casagrande device. A schematic diagram (side view) of a liquid limit device is shown in Figure 1.24a. This device consists of a brass cup and a hard rubber base. The brass cup can be dropped onto the base by a cam operated by a crank. To perform the liquid limit test, one must place a soil paste in the cup. A groove is then cut at the center of the soil pat with the standard grooving tool (Figure 1.24b). By using the crank-operated cam, the cup is lifted and dropped from a height of 10 mm. The moisture content, in percent, required to close a distance of 12.7 mm along the bottom of the groove (see Figure 1.24c and d) after 25 blows is defined as the *liquid limit*.

It is difficult to adjust the moisture content in the soil to meet the required 12.7 mm closure of the groove in the soil pat at 25 blows. Hence, at least

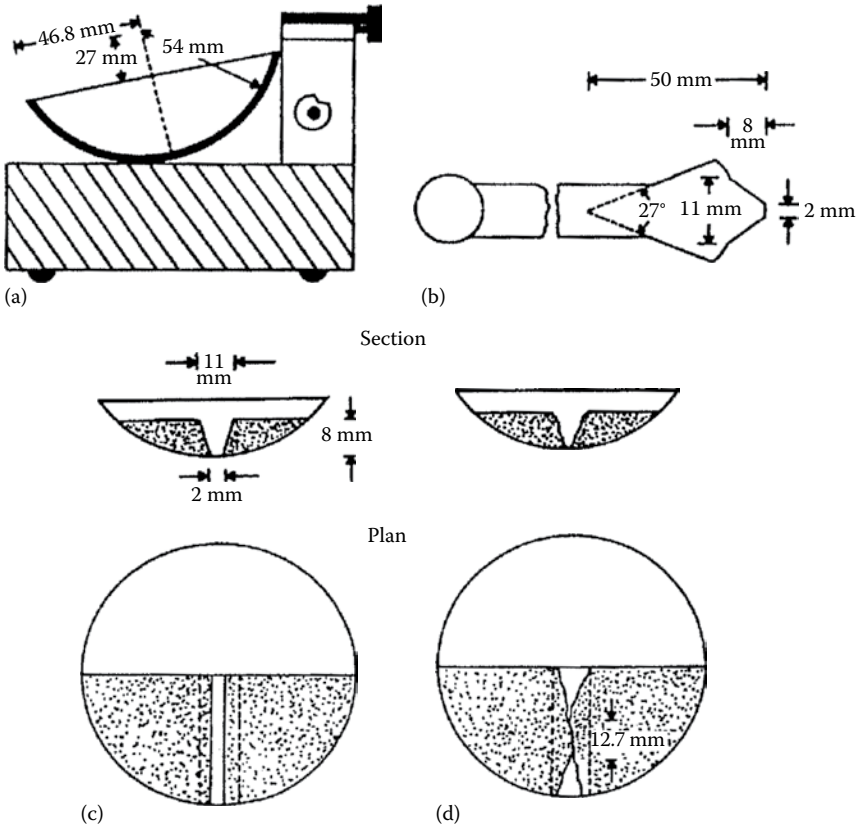

Figure 1.24 Schematic diagram of (a) liquid limit device, (b) grooving tool, (c) soil pat at the beginning of the test, and (d) soil pat at the end of the test.

three tests for the same soil are conducted at varying moisture contents, with the number of blows, N, required to achieve closure varying between 15 and 35. The moisture content of the soil, in percent, and the corresponding number of blows are plotted on semilogarithmic graph paper (Figure 1.25). The relationship between moisture content and log N is approximated as a straight line. This line is referred to as the *flow curve*. The moisture content corresponding to $N = 25$, determined from the flow curve, gives the liquid limit of the soil. The slope of the flow line is defined as the *flow index* and may be written as

$$I_F = \frac{w_1 - w_2}{\log(N_2/N_1)} \tag{1.15}$$

where

I_F is the flow index
w_1 is the moisture content of soil, in percent, corresponding to N_1 blows
w_2 is the moisture content corresponding to N_2 blows

Note that w_2 and w_1 are exchanged to yield a positive value even though the slope of the flow line is negative. Thus, the equation of the flow line can be written in a general form as

$$w = -I_F \log N + C \tag{1.16}$$

where C is a constant.

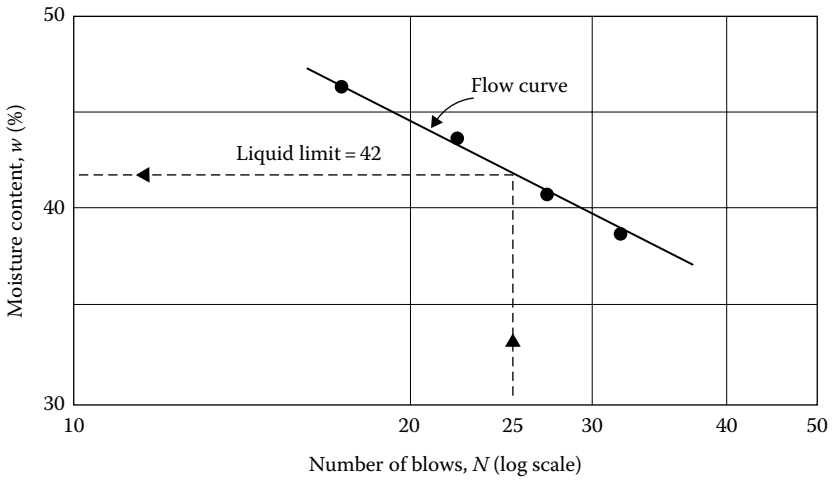

Figure 1.25 Flow curve for the determination of the liquid limit for a silty clay.

From the analysis of hundreds of liquid limit tests in 1949, the U.S. Army Corps of Engineers, at the Waterways Experiment Station in Vicksburg, Mississippi, proposed an empirical equation of the form

$$\mathrm{LL} = w_N \left(\frac{N}{25} \right)^{\tan\beta} \tag{1.17}$$

where

N is the number of blows in the liquid limit device for a 12.7 mm groove closure
w_N is the corresponding moisture content
$\tan\beta = 0.121$ (but note that $\tan\beta$ is not equal to 0.121 for all soils)

Equation 1.17 generally yields good results for the number of blows between 20 and 30. For routine laboratory tests, it may be used to determine the liquid limit when only one test is run for a soil. This procedure is generally referred to as the *one-point method* and was also adopted by ASTM under designation D-4318 (ASTM, 2014). The reason that the one-point method yields fairly good results is that a small range of moisture content is involved when $N = 20–30$.

Another method of determining the liquid limit, which is popular in Europe and Asia, is the *fall cone method* (British Standard—BS 1377). In this test, the liquid limit is defined as the moisture content at which a standard cone of apex angle 30° and weight of 0.78 N (80 gf) will penetrate a distance $d = 20$ mm in 5 s when allowed to drop from a position of point contact with the soil surface (Figure 1.26a). Due to the difficulty in achieving the liquid limit from a single test, four or more tests can be conducted at various moisture contents to determine the fall cone penetration, d, in 5 s. A semilogarithmic graph can then be plotted with moisture content w versus cone penetration d. The plot results in a straight line. The moisture content corresponding to $d = 20$ mm is the liquid limit (Figure 1.26b). From Figure 1.26b, the *flow index* can be defined as

$$I_{\mathrm{FC}} = \frac{w_2(\%) - w_1(\%)}{\log d_2 - \log d_1} \tag{1.18}$$

where w_1, w_2 are the moisture contents at cone penetrations of d_1 and d_2, respectively.

As in the case of the percussion cup method (ASTM D4318), attempts have been made to develop the estimation of liquid limit by a one-point method. They are

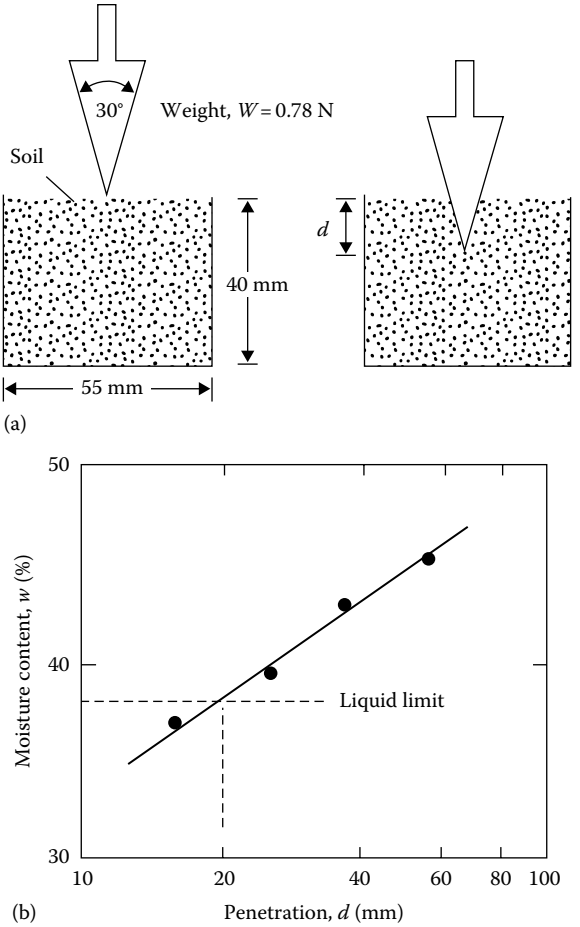

Figure 1.26 (a) Fall cone test and (b) plot of moisture content versus cone penetration for determination of liquid limit.

- Nagaraj and Jayadeva (1981)

$$\mathrm{LL} = \frac{w}{0.77 \log d} \tag{1.19}$$

$$\mathrm{LL} = \frac{w}{0.65 + 0.0175d} \tag{1.20}$$

- Feng (2001)

$$\mathrm{LL} = w\left(\frac{20}{d}\right)^{0.33} \tag{1.21}$$

Table 1.3 Summary of main differences among fall cones (Summarized from Budhu, 1985)

Country	*Cone details*	*Penetration for liquid limit (mm)*
Russia	Cone angle = 30° Cone mass = 76 g	10
Britain, France	Cone angle = 30° Cone mass = 80 g	20
India	Cone angle = 31° Cone mass = 148 g	20.4
Sweden, Canada (Québec)	Cone angle = 60° Cone mass = 60 g	10

Note: Duration of penetration is 5s in all cases.

where w (%) is the moisture content for a cone penetration d (mm) falling between 15 mm to 25 mm.

The dimensions of the cone tip angle, cone weight, and the penetration (mm) at which the liquid limit is determined varies from country to country. Table 1.3 gives a summary of different fall cones used in various countries.

A number of major studies have shown that the undrained shear strength of the soil at liquid limit varies between 1.7 and 2.3 kN/m^2. Based on tests conducted on a large number of soil samples, Feng (2001) has given the following correlation between the liquid limits determined according to ASTM D4318 and British Standard BS1377.

$$LL_{(BS)} = 2.6 + 0.94[LL_{(ASTM)}] \tag{1.22}$$

Example 1.1

One liquid limit test was conducted on a soil using the fall cone. Following are the results: $w = 29.5\%$ at $d = 15$ mm. Estimate the liquid limit of the soil using Equations 1.19, 1.20, and 1.21.

Solution

From Equation 1.19,

$$LL = \frac{w}{0.77 \log d} = \frac{29.5}{(0.77)(\log 15)} = \mathbf{32.58}$$

From Equation 1.20,

$$LL = \frac{w}{0.65 + 0.0175d} = \frac{29.5}{0.65 + (0.0175)(15)} = \mathbf{32.33}$$

From Equation 1.21,

$$\text{LL} = w\left(\frac{20}{d}\right)^{0.33} = (29.5)\left(\frac{20}{15}\right)^{0.33} = \mathbf{32.43}$$

1.8.2 Plastic limit

The *plastic limit* is defined as the moist content, in percent, at which the soil crumbles when rolled into threads of 3.2 mm diameter. The plastic limit is the lower limit of the plastic stage of soil. The plastic limit test is simple and is performed by repeated rolling of an ellipsoidal size soil mass by hand on a ground glass plate. The procedure for the plastic limit test is given by ASTM Test Designation D-4318 (ASTM, 2014).

As in the case of liquid limit determination, the fall cone method can be used to obtain the plastic limit. This can be achieved by using a cone of similar geometry, but with a mass of 2.35 N (240 gf). Three to four tests at varying moist contents of soil are conducted, and the corresponding cone penetrations d are determined. The moisture content corresponding to a cone penetration of d = 20 mm is the plastic limit. Figure 1.27 shows the liquid and plastic limit determined by the fall cone test for Cambridge Gault clay reported by Wroth and Wood (1978).

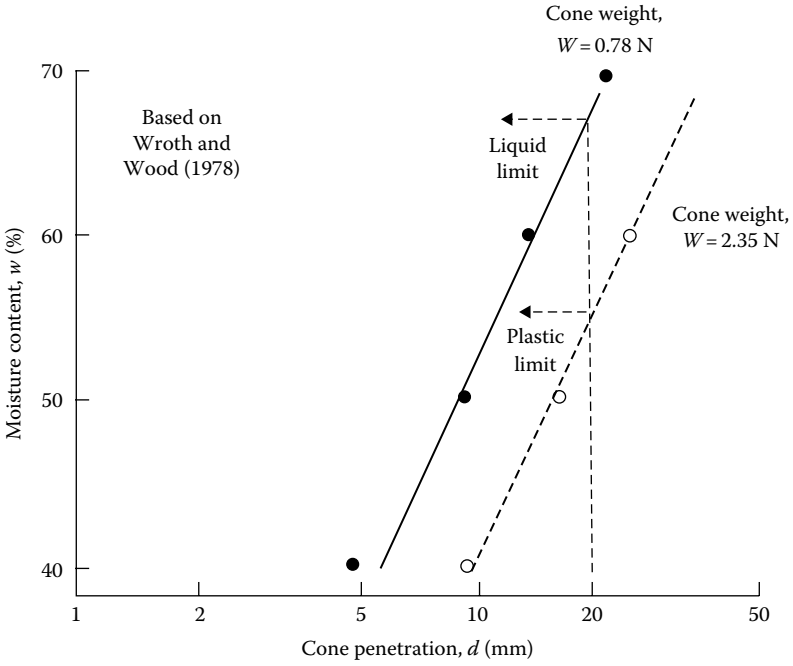

Figure 1.27 Liquid and plastic limits for Cambridge Gault clay determined by the fall cone test.

The difference between the liquid limit and the plastic limit of a soil is defined as the plasticity index, PI

$$\text{PI} = \text{LL} - \text{PL} \tag{1.23}$$

where
LL is the liquid limit
PL is the plastic limit

Sridharan et al. (1999) showed that the plasticity index can be correlated to the flow index as obtained from the liquid limit tests. According to their study

$$\text{PI}(\%) = 4.12 I_{\text{F}}(\%) \tag{1.24}$$

and

$$\text{PI}(\%) = 0.74 I_{\text{FC}}(\%) \tag{1.25}$$

1.9 LIQUIDITY INDEX

The relative consistency of a cohesive soil can be defined by a ratio called the *liquidity index* LI. It is defined as

$$\text{LI} = \frac{w_{\text{N}} - \text{PL}}{\text{LL} - \text{PL}} = \frac{w_{\text{N}} - \text{PL}}{\text{PI}} \tag{1.26}$$

where w_{N} is the natural moisture content. It can be seen from Equation 1.26 that, if w_{N} = LL, then the liquidity index is equal to 1. Again, if w_{N} = PL, the liquidity index is equal to 0. Thus, for a natural soil deposit which is in a plastic state (i.e., LL $\geq w_{\text{N}} \geq$ PL), the value of the liquidity index varies between 1 and 0. A natural deposit with $w_{\text{N}} \geq$ LL will have a liquidity index greater than 1. In an undisturbed state, these soils may be stable; however, a sudden shock may transform them into a liquid state. Such soils are called *sensitive clays*.

1.10 ACTIVITY

Since the plastic property of soil is due to the adsorbed water that surrounds the clay particles, we can expect that the type of clay minerals and their proportional amounts in a soil will affect the liquid and plastic limits. Skempton (1953) observed that the plasticity index of a

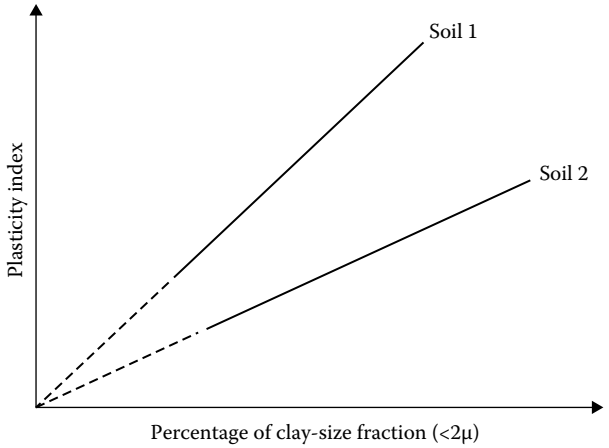

Figure 1.28 Relationship between plasticity index and percentage of clay-size fraction by weight.

soil linearly increases with the percent of clay-size fraction (percent finer than 2μ by weight) present in it. This relationship is shown in Figure 1.28. The average lines for all the soils pass through the origin. The correlations of PI with the clay-size fractions for different clays plot separate lines. This is due to the type of clay minerals in each soil. On the basis of these results, Skempton defined a quantity called activity, which is the slope of the line correlating PI and percent finer than 2μ. This activity A may be expressed as

$$A = \frac{\text{PI}}{(\text{percentage of clay-size fraction by weight})} \tag{1.27}$$

Activity is used as an index for identifying the swelling potential of clay soils. Typical values of activities for various clay minerals are given in Table 1.4.

Table 1.4 Activities of clay minerals

Mineral	*Activity (A)*
Smectites	1–7
Illite	0.5–1
Kaolinite	0.5
Halloysite ($4H_2O$)	0.5
Halloysite ($2H_2O$)	0.1
Attapulgite	0.5–1.2
Allophane	0.5–1.2

Seed et al. (1964a) studied the plastic property of several artificially prepared mixtures of sand and clay. They concluded that, although the relationship of the plasticity index to the percent of clay-size fraction is linear (as observed by Skempton), it may not always pass through the origin. This is shown in Figure 1.29. Thus, the activity can be redefined as

$$A = \frac{\text{PI}}{\text{percent of clay-size fraction} - C'} \tag{1.28}$$

where C' is a constant for a given soil. For the experimental results shown in Figure 1.29, $C' = 9$.

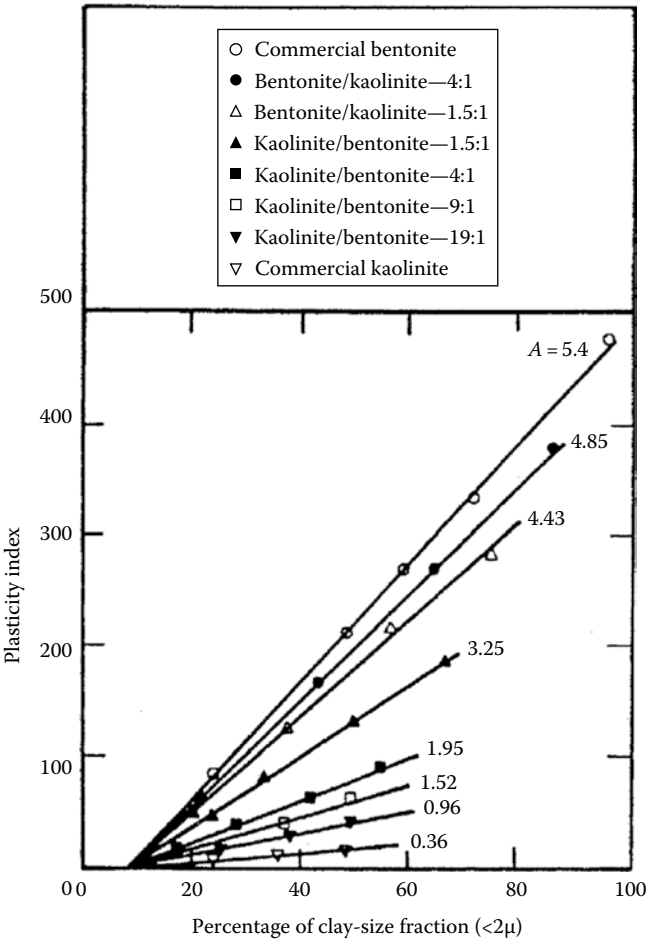

Figure 1.29 Relationship between plasticity index and clay-size fraction by weight for kaolinite/bentonite clay mixtures. [After Seed, H. B. et al., *J. Soil Mech. Found. Eng. Div.*, ASCE, 90(SM4), 107, 1964.]

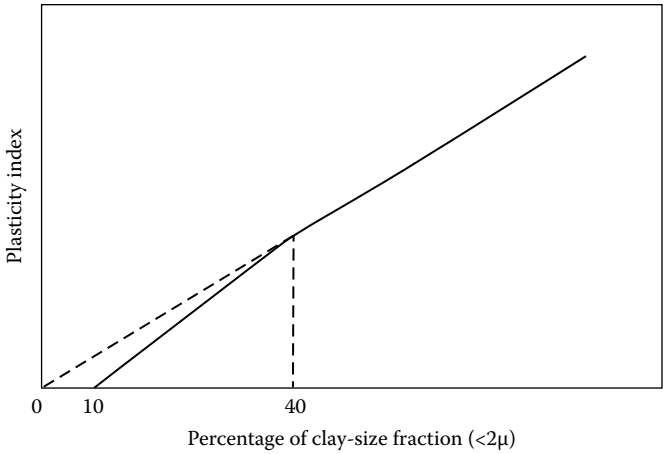

Figure 1.30 Simplified relationship between plasticity index and percentage of clay-size fraction by weight. [After Seed, H. B. et al., *J. Soil Mech. Found. Eng. Div.*, ASCE, 90(SM6), 75, 1964.]

Further works of Seed et al. (1964b) have shown that the relationship of the plasticity index to the percentage of clay-size fractions present in a soil can be represented by two straight lines. This is shown qualitatively in Figure 1.30. For clay-size fractions greater than 40%, the straight line passes through the origin when it is projected back.

1.11 GRAIN-SIZE DISTRIBUTION OF SOIL

For a basic understanding of the nature of soil, the distribution of the grain size present in a given soil mass must be known. The grain-size distribution of coarse-grained soils (gravelly and/or sandy) is determined by sieve analysis. Table 1.5 gives the opening size of some U.S. sieves.

The cumulative percent by weight of a soil passing a given sieve is referred to as the *percent finer*. Figure 1.31 shows the results of a sieve analysis for a sandy soil. The grain-size distribution can be used to determine some of the basic soil parameters, such as the effective size, the uniformity coefficient, and the coefficient of gradation.

The *effective size* of a soil is the diameter through which 10% of the total soil mass is passing and is referred to as D_{10}. The *uniformity coefficient* C_u is defined as

$$C_u = \frac{D_{60}}{D_{10}} \tag{1.29}$$

where D_{60} is the diameter through which 60% of the total soil mass is passing.

Table 1.5 U.S. standard sieves

Sieve no.	*Opening size (mm)*
3	6.35
4	4.75
6	3.36
8	2.38
10	2.00
16	1.19
20	0.84
30	0.59
40	0.425
50	0.297
60	0.25
70	0.21
100	0.149
140	0.105
200	0.075
270	0.053

The *coefficient of gradation* C_c is defined as

$$C_c = \frac{(D_{30})^2}{(D_{60})(D_{10})} \tag{1.30}$$

where D_{30} is the diameter through which 30% of the total soil mass is passing.

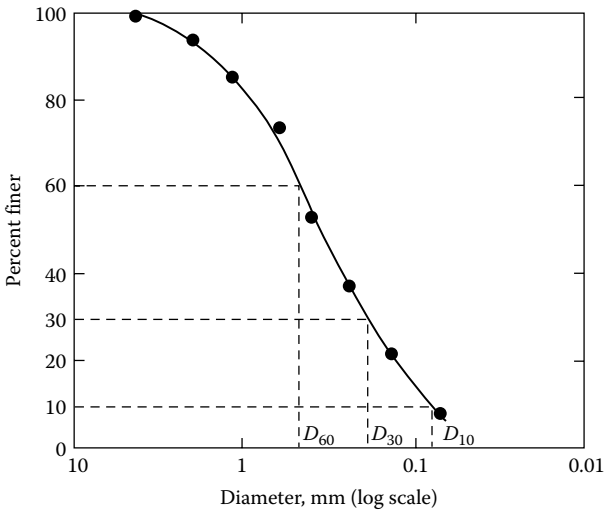

Figure 1.31 Grain-size distribution of a sandy soil.

A soil is called a *well-graded* soil if the distribution of the grain sizes extends over a rather large range. In that case, the value of the uniformity coefficient is large. Generally, a soil is referred to as well graded if C_u is larger than about 4–6 and C_c is between 1 and 3. When most of the grains in a soil mass are of approximately the same size—that is, C_u is close to 1—the soil is called *poorly graded*. A soil might have a combination of two or more well-graded soil fractions, and this type of soil is referred to as a *gap-graded* soil.

The sieve analysis technique described earlier is applicable for soil grains larger than No. 200 (0.075 mm) sieve size. For fine-grained soils, the procedure used for determination of the grain-size distribution is hydrometer analysis. This is based on the principle of sedimentation of soil grains.

1.12 WEIGHT–VOLUME RELATIONSHIPS

Figure 1.32a shows a soil mass that has a total volume V and a total weight W. To develop the weight–volume relationships, the three phases of the soil mass, that is, soil solids, air, and water, have been separated in Figure 1.32b. Note that

$$W = W_s + W_w \tag{1.31}$$

and, also

$$V = V_s + V_w + V_a \tag{1.32}$$

$$V_v = V_w + V_a \tag{1.33}$$

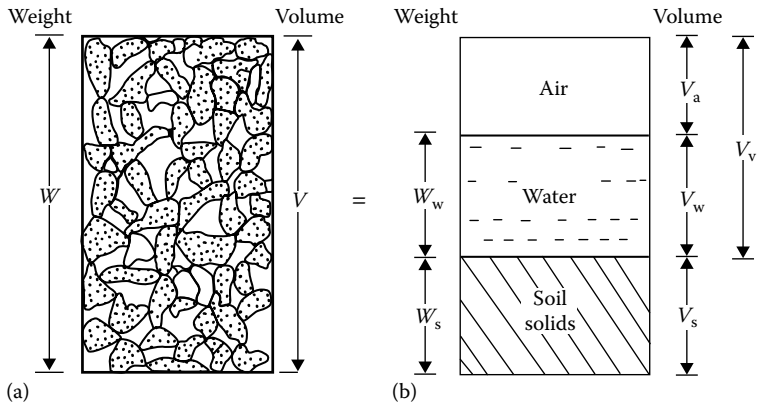

Figure 1.32 Weight–volume relationships for soil aggregate: (a) soil mass of volume V; (b) three phases of the soil mass.

where

W_s is the weight of soil solids
W_w is the weight of water
V_s is the volume of the soil solids
V_w is the volume of water
V_a is the volume of air

The weight of air is assumed to be zero. The volume relations commonly used in soil mechanics are void ratio, porosity, and degree of saturation.

Void ratio e is defined as the ratio of the volume of voids to the volume of solids:

$$e = \frac{V_v}{V_s} \tag{1.34}$$

Porosity n is defined as the ratio of the volume of voids to the total volume:

$$n = \frac{V_v}{V} \tag{1.35}$$

Also, $V = V_s + V_v$
and so

$$n = \frac{V_v}{V_s + V_v} = \frac{V_v/V_s}{(V_s/V_s) + (V_v/V_s)} = \frac{e}{1+e} \tag{1.36}$$

Degree of saturation S_r is the ratio of the volume of water to the volume of voids and is generally expressed as a percentage:

$$S_r(\%) = \frac{V_w}{V_v} \times 100 \tag{1.37}$$

The weight relations used are moisture content and unit weight. *Moisture content w* is defined as the ratio of the weight of water to the weight of soil solids, generally expressed as a percentage:

$$w(\%) = \frac{W_w}{W_s} \times 100 \tag{1.38}$$

Unit weight γ is the ratio of the total weight to the total volume of the soil aggregate:

$$\gamma = \frac{W}{V} \tag{1.39}$$

This is sometimes referred to as moist unit weight since it includes the weight of water and the soil solids. If the entire void space is filled with water (i.e., $V_a = 0$), it is a saturated soil; Equation 1.39 will then give us the saturated unit weight γ_{sat}.

The dry unit weight γ_d is defined as the ratio of the weight of soil solids to the total volume:

$$\gamma_d = \frac{W_s}{V} \tag{1.40}$$

Useful weight–volume relations can be developed by considering a soil mass in which the volume of soil solids is unity, as shown in Figure 1.33. Since $V_s = 1$, from the definition of void ratio given in Equation 1.34, the volume of voids is equal to the void ratio e. The weight of soil solids can be given by

$$W_s = G_s\gamma_w V_s = G_s\gamma_w \quad (\text{since} V_s = 1)$$

where

G_s is the specific gravity of soil solids

γ_w is the unit weight of water (9.81 kN/m^3)

From Equation 1.38, the weight of water is $W_w = wW_s = wG_s\gamma_w$. So the moist unit weight is

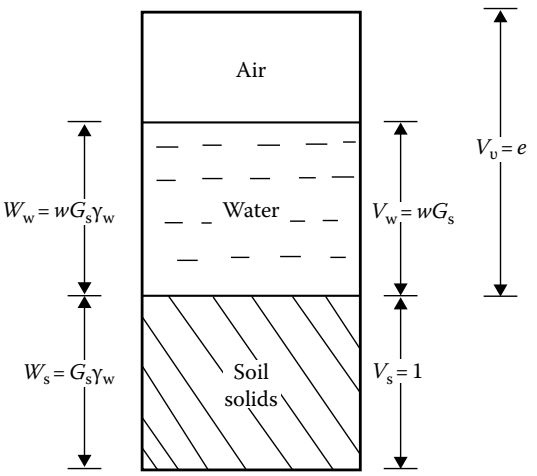

Figure 1.33 Weight–volume relationship for V_s = 1.

$$\gamma = \frac{W}{V} = \frac{W_s + W_w}{V_s + V_v} = \frac{G_s\gamma_w + wG_s\gamma_w}{1+e} = \frac{G_s\gamma_w(1+w)}{1+e} \tag{1.41}$$

The dry unit weight can also be determined from Figure 1.33 as

$$\gamma_d = \frac{W_s}{V} = \frac{G_s\gamma_w}{1+e} \tag{1.42}$$

The degree of saturation can be given by

$$S_r = \frac{V_w}{V_v} = \frac{W_w/\gamma_w}{V_v} = \frac{wG_s\gamma_w/\gamma_w}{e} = \frac{wG_s}{e} \tag{1.43}$$

For saturated soils, $S_r = 1$. So, from Equation 1.43,

$$e = wG_s \tag{1.44}$$

By referring to Figure 1.34, the relation for the unit weight of a saturated soil can be obtained as

$$\gamma_{sat} = \frac{W}{V} = \frac{W_s + W_w}{V} = \frac{G_s\gamma_w + e\gamma_w}{1+e} \tag{1.45}$$

Basic relations for unit weight such as Equations 1.41, 1.42, and 1.45 in terms of porosity n can also be derived by considering a soil mass that has a total volume of unity as shown in Figure 1.35. In this case (for $V = 1$), from Equation 1.35, $V_v = n$. So, $V_s = V - V_v = 1 - n$.

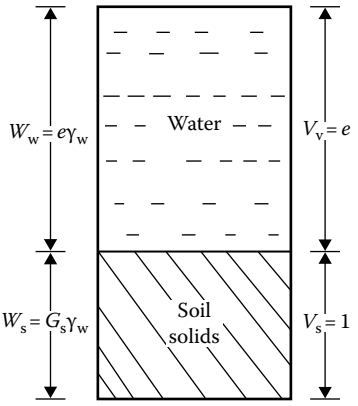

Figure 1.34 Weight–volume relation for saturated soil with $V_s = 1$.

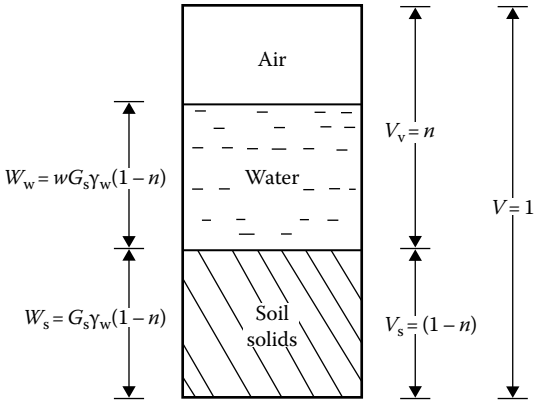

Figure 1.35 Weight–volume relationship for $V = 1$.

The weight of soil solids is equal to $(1 - n)G_s\gamma_w$, and the weight of water $W_w = wW_s = w(1 - n)G_s\gamma_w$. Thus, the moist unit weight is

$$\gamma = \frac{W}{V} = \frac{W_s + W_w}{V} = \frac{(1-n)G_s\gamma_w + w(1-n)G_s\gamma_w}{1}$$

$$= G_s\gamma_w(1-n)(1+w) \tag{1.46}$$

The dry unit weight is

$$\gamma_d = \frac{W_s}{V} = (1-n)G_s\gamma_w \tag{1.47}$$

If the soil is saturated (Figure 1.36),

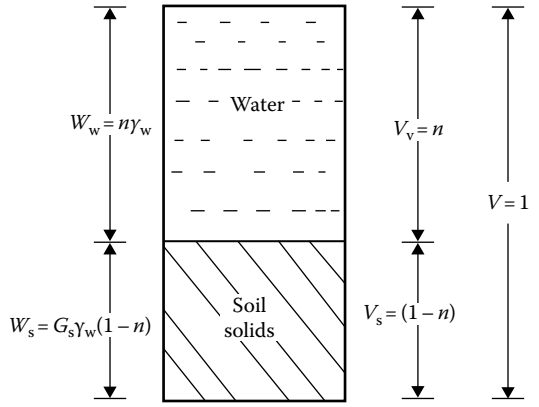

Figure 1.36 Weight–volume relationship for saturated soil with $V = 1$.

Table 1.6 Typical values of void ratios and dry unit weights for granular soils

	Void ratio, e		*Dry unit weight, γ_d*	
Soil type	*Maximum*	*Minimum*	*Minimum (kN/m³)*	*Maximum (kN/m³)*
Gravel	0.6	0.3	16	20
Coarse sand	0.75	0.35	15	19
Fine sand	0.85	0.4	14	19
Standard Ottawa sand	0.8	0.5	14	17
Gravelly sand	0.7	0.2	15	22
Silty sand	1	0.4	13	19
Silty sand and gravel	0.85	0.15	14	23

$$\gamma_{sat} = \frac{W_s + W_w}{V} = (1-n)G_s\gamma_w + n\gamma_w = [G_s - n(G_s - 1)]\gamma_w \tag{1.48}$$

Table 1.6 gives some typical values of void ratios and dry unit weights encountered in granular soils.

Example 1.2

For a soil in natural state, given $e = 0.8$, $w = 24\%$, and $G_s = 2.68$.

a. Determine the moist unit weight, dry unit weight, and degree of saturation.
b. If the soil is completely saturated by adding water, what would its moisture content be at that time? Also, find the saturated unit weight.

Solution

Part a:

From Equation 1.41, the moist unit weight is

$$\gamma = \frac{G_s\gamma_w(1+w)}{1+e}$$

Since $\gamma_w = 9.81$ kN/m³,

$$\gamma = \frac{(2.68)(9.81)(1+0.24)}{1+0.8} = 18.11\,\text{kN/m}^3$$

From Equation 1.42, the dry unit weight is

$$\gamma_d = \frac{G_s\gamma_w}{1+e} = \frac{(2.68)(9.81)}{1+0.8} = 14.61\,\text{kN/m}^3$$

From Equation 1.43, the degree of saturation is

$$S_r(\%) = \frac{wG_s}{e} \times 100 = \frac{(0.24)(2.68)}{0.8} \times 100 = 80.4\%$$

Part b:

From Equation 1.44, for saturated soils, $e = wG_s$, or

$$w(\%) = \frac{e}{G_s} \times 100 = \frac{0.8}{2.68} \times 100 = 29.85\%$$

From Equation 1.45, the saturated unit weight is

$$\gamma_{sat} = \frac{G_s\gamma_w + e\gamma_w}{1+e} = \frac{9.81(2.68+0.8)}{1+0.8} = 18.97\ \text{kN/m}^3$$

Example 1.3

In the natural state, a moist soil has a volume of 0.0093 m^3 and weighs 177.6 N. The oven dry weight of the soil is 153.6 N. If $G_s = 2.71$, calculate the moisture content, moist unit weight, dry unit weight, void ratio, porosity, and degree of saturation.

Solution

Refer to Figure 1.37. The moisture content (Equation 1.38) is

$$w = \frac{W_w}{W_s} = \frac{W - W_s}{W_s} = \frac{177.6 - 153.6}{153.6} = \frac{24}{153.6} \times 100 = \mathbf{15.6\%}$$

The moist unit weight (Equation 1.39) is

$$\gamma = \frac{W}{V} = \frac{177.6}{0.0093} = 19{,}096\ \text{N/m}^3 \approx \mathbf{19.1\ kN/m^3}$$

For dry unit weight (Equation 1.40), we have

$$\gamma_d = \frac{W_s}{V} = \frac{153.6}{0.0093} = 16{,}516\ \text{N/m}^3 \approx \mathbf{16.52\ kN/m^3}$$

The void ratio (Equation 1.34) is found as follows:

$$e = \frac{V_v}{V_s}$$

$$V_s = \frac{W_s}{G_s\gamma_w} = \frac{0.1536}{2.71 \times 9.81} = 0.0058\ \text{m}^3$$

$$V_v = V - V_s = 0.0093 - 0.0058 = 0.0035\ \text{m}^3$$

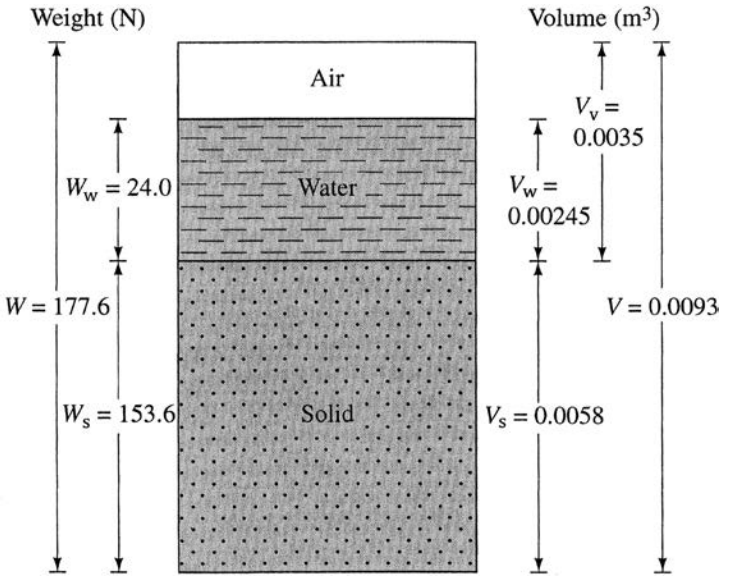

Figure 1.37 Three phases of a soil sample.

So

$$e = \frac{0.0035}{0.0058} \approx \mathbf{0.60}$$

For porosity (Equation 1.36), we have

$$n = \frac{e}{1+e} = \frac{0.60}{1+0.60} = \mathbf{0.375}$$

We find the degree of saturation (Equation 1.37) as follows:

$$S = \frac{V_w}{V_v}$$

$$V_w = \frac{W_w}{\gamma_w} = \frac{0.024}{9.81} = 0.00245 \text{ m}^3$$

So

$$S = \frac{0.00245}{0.0035} \times 100 = \mathbf{70\%}$$

Example 1.4

For a saturated soil, show that

$$\gamma_{sat} = \left(\frac{e}{w}\right)\left(\frac{1+w}{1+e}\right)\gamma_w.$$

Solution

From Equations 1.44 and 1.45,

$$\gamma_{sat} = \frac{(G_s + e)\gamma_w}{1+e} \tag{a}$$

and

$$e = wG_s$$

or

$$G_s = \frac{e}{w} \tag{b}$$

Combining Equations (a) and (b) gives

$$\gamma_{sat} = \frac{\left(\frac{e}{w} + e\right)\gamma_w}{1+e} = \left(\frac{e}{w}\right)\left(\frac{1+w}{1+e}\right)\gamma_w$$

1.13 RELATIVE DENSITY AND RELATIVE COMPACTION

Relative density is a term generally used to describe the degree of compaction of coarse-grained soils. Relative density D_r is defined as

$$D_r = \frac{e_{max} - e}{e_{max} - e_{min}} \tag{1.49}$$

where

e_{max} is the maximum possible void ratio
e_{min} is the minimum possible void ratio
e is the void ratio in natural state of soil

Equation 1.49 can also be expressed in terms of dry unit weight of the soil:

$$\gamma_d(\text{max}) = \frac{G_s\gamma_w}{1+e_{min}} \quad \text{or} \quad e_{min} = \frac{G_s\gamma_w}{\gamma_d(\text{max})} - 1 \tag{1.50}$$

Similarly,

$$e_{max} = \frac{G_s \gamma_w}{\gamma_d(\min)} - 1 \tag{1.51}$$

and

$$e = \frac{G_s \gamma_w}{\gamma_d} - 1 \tag{1.52}$$

where $\gamma_d(\max)$, $\gamma_d(\min)$, and γ_d are the maximum, minimum, and natural-state dry unit weights of the soil. Substitution of Equations 1.50 through 1.52 into Equation 1.49 yields

$$D_r = \left[\frac{\gamma_d(\max)}{\gamma_d}\right]\left[\frac{\gamma_d - \gamma_d(\min)}{\gamma_d(\max) - \gamma_d(\min)}\right] \tag{1.53}$$

Relative density is generally expressed as a percentage. It has been used by several investigators to correlate the angle of friction of soil, the soil liquefaction potential, etc.

Another term occasionally used in regard to the degree of compaction of coarse-grained soils is *relative compaction*, R_c, which is defined as

$$R_c = \frac{\gamma_d}{\gamma_d(\max)} \tag{1.54a}$$

Comparing Equations 1.53 and 1.54a,

$$R_c = \frac{R_o}{1 - D_r(1 - R_o)} \tag{1.54b}$$

where $R_o = \gamma_d(\min)/\gamma_d(\max)$.

Lee and Singh (1971) reviewed 47 different soils and gave the approximate relation between relative compaction and relative density as

$$R_c = 80 + 0.2D_r \tag{1.54c}$$

where D_r is in percent.

1.13.1 Correlations for relative density of granular soil

Several correlations have been proposed for estimation of relative density from standard penetration test results obtained from field soil exploration programs. Some of those relationships are given below.

Kulhawy and Mayne (1990) modified an empirical relationship for relative density that was given by Marcuson and Bieganousky (1977), which can be expressed as

$$D_r(\%) = 12.2 + 0.75\left[222N_{60} + 2311 - 711\text{OCR} - 779\left(\frac{\sigma'_o}{p_a}\right) - 50C_u^2\right]^{0.5} \tag{1.55}$$

where

D_r = relative density
N_{60} = standard penetration number for an energy ratio of 60%
σ'_o = effective overburden pressure
C_u = uniformity coefficient of sand

$$\text{OCR} = \frac{\text{preconsolidation pressure, } \sigma'_c}{\text{effective overburden pressure, } \sigma'_o}$$

p_a = atmospheric pressure (≈100 kN/m²)

Meyerhof (1957) developed a correlation between D_r and N_{60} as

$$N_{60} = \left[17 + 24\left(\frac{\sigma'_o}{p_a}\right)\right]D_r^2$$

or

$$D_r = \left\{\frac{N_{60}}{\left[17 + 24\left(\frac{\sigma'_o}{p_a}\right)\right]}\right\}^{0.5} \tag{1.56}$$

Equation 1.56 provides a reasonable estimate only for clean, medium fine sand.

Cubrinovski and Ishihara (1999) also proposed a correlation between N_{60} and the relative density of sand (D_r) that can be expressed as

$$D_r(\%) = \left[\frac{N_{60}\left(0.23 + \frac{0.06}{D_{50}}\right)^{1.7}}{9}\left(\frac{1}{\frac{\sigma'_o}{p_a}}\right)\right]^{0.5} (100) \tag{1.57}$$

where

p_a = atmospheric pressure (≈100 kN/m²)
D_{50} = sieve size through which 50% of the soil will pass (mm)

Kulhawy and Mayne (1990) correlated the corrected standard penetration number and the relative density of sand in the form

$$D_r(\%) = \left[\frac{(N_1)_{60}}{C_p C_A C_{OCR}}\right]^{0.5} (100) \tag{1.58}$$

where

$$C_p = \text{grain-size correlations factor} = 60 + 25\log D_{5(} \tag{1.59}$$

$$C_A = \text{correlation factor for aging} = 1.2 + 0.05\log\left(\frac{t}{100}\right) \tag{1.60}$$

$$C_{OCR} = \text{correlation factor for overconsolidation} = \text{OCR}^{0.18} \tag{1.61}$$

D_{50} = diameter through which 50% of the soil will pass (mm)
t = age of soil since deposition (years)
OCR = overconsolidation ratio

Skempton (1986) suggested that, for sand with a relative density greater than 35%,

$$\frac{(N_1)_{60}}{D_r^2} \approx 60 \tag{1.62}$$

where $(N_1)_{60}$ is N_{60} corrected to an effective overburden pressure of $p_a \approx 100$ kN/m^2. $(N_1)_{60}$ should be multiplied by 0.92 for coarse sands and 1.08 for fine sands.

More recently Mujtaba et al. (2017) have provided the following correlation for D_r:

$$D_r(\%) = 1.96N_{60} - 19.2\left(\frac{p_a}{\sigma'_o}\right)^{0.23} + 29.2 \tag{1.63}$$

For more details of N_{60} and $(N_1)_{60}$, the readers are referred to Das (2016).

1.14 RELATIONSHIP BETWEEN e_{max} AND e_{min}

The maximum and minimum void ratios for granular soils described in Section 1.13 depend on several factors such as

- Grain size
- Grain shape

- Nature of grain-size distribution
- Fine content F_c (i.e., fraction smaller than 0.075 mm)

Following are some of the correlations now available in the literature related to e_{max} and e_{min} of granular soils.

- Clean sand (F_c = 0%–5%)

Miura et al. (1997) conducted an extensive study of the physical characteristics of about 200 samples of granular material, which included mostly clean sand, some glass beads, and lightweight aggregates (LWA). Figure 1.38 shows a plot of e_{max} versus e_{min} obtained from that study, which shows that

$$e_{max} \approx 1.62 e_{min} \tag{1.64}$$

Cubrinovski and Ishihara (2002) analyzed a large number of clean sand samples based on which it was suggested that

$$e_{max} = 0.072 + 1.53 e_{min} \tag{1.65}$$

Based on best-fit linear regression lines, Cubrinovski and Ishihara (2002) also provided the following relationships for other soils:

- Sand with fines (5% < $F_c \leq$ 15%)

$$e_{max} = 0.25 + 1.37 e_{min} \tag{1.66}$$

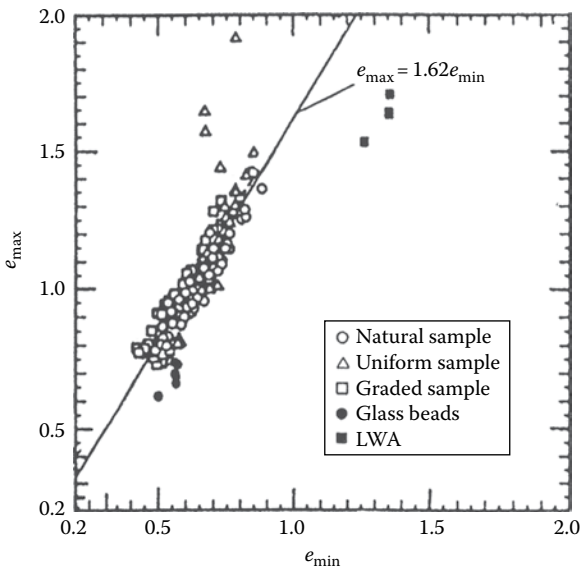

Figure 1.38 Plot of e_{max} versus e_{min} based on the results of Miura et al. (1997).

- Sand with fines and clay ($15\% < F_c \leq 30\%$; $P_c = 5\%–20\%$)

$$e_{max} = 0.44 + 1.21 e_{min} \tag{1.67}$$

- Silty soils ($30\% < F_c \leq 70\%$; $P_c = 5\%–20\%$)

$$e_{max} = 0.44 + 1.32 e_{min} \tag{1.68}$$

where
F_c is the fine fraction for which grain size is smaller than 0.075 mm
P_c is the clay-size fraction (<0.005 mm)

With a very large database, Cubrinovski and Ishihara (1999, 2002) developed a unique relationship between $e_{max} - e_{min}$ and median grain size D_{50}. The database included results from clean sand, sand with fines, and sand with clay, silty soil, gravelly sand, and gravel. This relationship is shown in Figure 1.39. In spite of some scatter, the average line can be given by the relation

$$e_{max} - e_{min} = 0.23 + \frac{0.06}{D_{50}(\text{mm})} \tag{1.69}$$

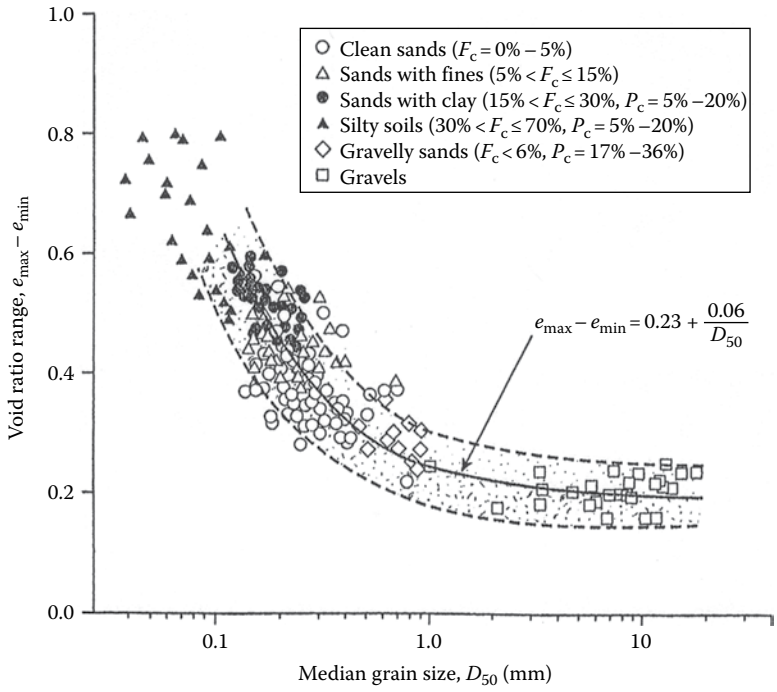

Figure 1.39 Plot of $e_{max} - e_{min}$ versus median grain size (D_{50}). [Redrawn after Cubrinovski and Ishihara, *Soils Found.*, 42(6), 65–78, 2002.]

It appears that the upper and lower limits of $e_{max} - e_{min}$ versus D_{50} as shown in Figure 1.39 can be approximated as

- Lower limit

$$e_{max} - e_{min} = 0.16 + \frac{0.045}{D_{50}(\text{mm})} \tag{1.70}$$

- Upper limit

$$e_{max} - e_{min} = 0.29 + \frac{0.079}{D_{50}(\text{mm})} \tag{1.71}$$

Youd (1973) analyzed the variation of e_{max} and e_{min} of several sand samples and provided relationships between angularity A of sand particles and the uniformity coefficient ($C_u = D_{60}/D_{10}$). The angularity, A, of a granular soil particle is defined as

$$A = \frac{\text{Average radius of corners and edges}}{\text{Radius of maximum inscribed sphere}} \tag{1.72}$$

For further details on angularity the readers may refer to Das and Sobhan (2018).

The qualitative descriptions of sand particles with the range of angularity as provided by Youd (1973) are given below.

- **Very angular**—The particles that have unworn fractured surfaces and multiple sharp corners and edges. The value of A varies within a range of 0.12–0.17 with a mean value of 0.14.
- **Angular**—The particles with sharp corners having prismoidal or tetrahedral shapes with $A = 0.17–0.25$ with a mean value of 0.21.
- **Sub-angular**—The particles have blunted or slightly rounded corners and edges with $A = 0.25–0.35$ with a mean value of about 0.30.
- **Sub-rounded**—The particles have well-rounded edges and corners. The magnitude of A varies in the range of 0.35–0.49 with a mean value of 0.41.
- **Rounded**—The particles are irregularly shaped and rounded with no distinct corners or edges for which $A = 0.49–0.79$ with a mean value of 0.59.
- **Well-rounded**—The particles have a spherical or ellipsoidal shape with $A = 0.7–1.0$ with a mean value of about 0.48.

The variations of e_{max} and e_{min} with criteria described above are given in Figure 1.40. Note that, for a given value of C_u, the maximum and minimum void ratios increase with the decrease in angularity. Also, for a given value of A, the magnitudes of e_{max} and e_{min} decrease with an increase in C_u.

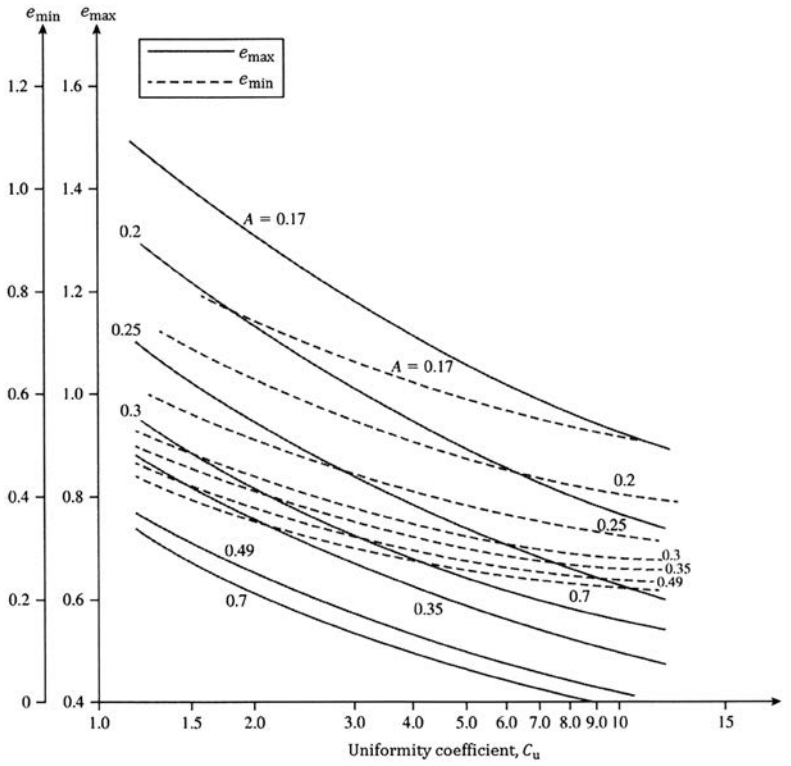

Figure 1.40 Variation of e_{max} and e_{min} with A and C_u. (Adapted from Youd, T. L., Factors controlling maximum and minimum densities of sand, *Evaluation of Relative Density and Its Role in Geotechnical Projects Involving Cohesionless Soils*, STP 523, ASTM, 98–122, 1973.)

1.14.1 Effect of nonplastic fines on e_{max} and e_{min}

The amount of *nonplastic fines* present in a given granular soil has a great influence on e_{max} and e_{min}. In order to visualize this, let us consider the study of McGeary (1961) related to the determination of the minimum void ratio (e_{min}) for idealized spheres (also see Lade et al., 1998). McGeary (1961) conducted tests with mixtures of two different sizes of steel spheres. The larger spheres had a diameter (D) of 3.15 mm. The diameter of the small spheres (d) varied from 0.91 mm to 0.15 mm. This provided a D/d ratio in the range of 3.45 to 19.69. Figure 1.41 shows the variation of e_{min} with the percent of small spheres in the mixture by volume for $D/d = 3.45$ and 4.77. For a given D/d value, the magnitude of e_{min} decreases with the increase in the volume of small spheres to an absolute minimum value $e_{min(min)}$. This occurs when the volume of small spheres in the mix is V_F. Beyond this point, the magnitude of e_{min} increases with the increase in the volume of smaller spheres.

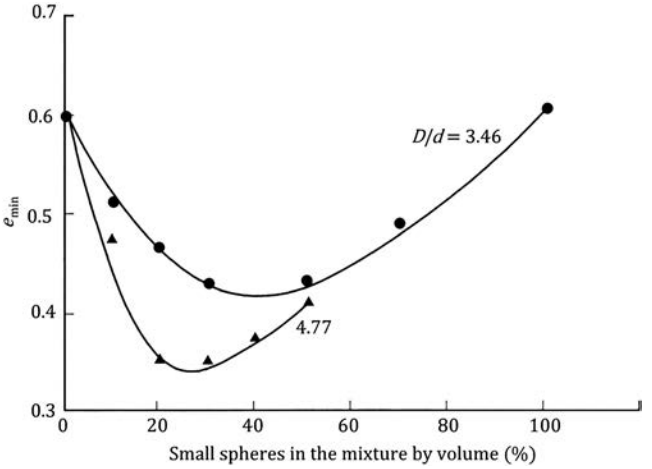

Figure 1.41 Test results of McGeary (1961)—Variation of minimum void ratio with percent of smaller steel spheres by volume.

Table 1.7 provides a summary of all of the test results of McGeary (1961). This is also shown in Figure 1.42, from which it can be concluded that (a) for $D/d \geq 7$, the magnitude of $e_{min(min)}$ remains approximately constant ($\approx$0.2), and (b) at $e_{min(min)}$, the approximate magnitude of $V_F \approx 27\%$.

In order to compare the preceding experimental results with idealized spheres with the actual soil, we consider the study of Lade et al. (1998), which was conducted with two types: Nevada sand (retained on No. 200 U.S. sieve) and Nevada nonplastic fines (passing No. 200 U.S. sieve). Table 1.8 shows the D_{50} (size through 50% soil will pass) for the two sands and the nonplastic fines. Figure 1.43 shows the variation of e_{max} and e_{min} with percent of fines by volume. From this figure it can be seen that:

Table 1.7 Interpolated values of $e_{min(min)}$ from binary packing based on the tests of McGeary (1961)

D/d	$e_{min(min)}$	*Approximate volume of small spheres at which* $e_{min(min)}$ *occurs,* V_F *(%)*
3.46	0.426	41.3
4.77	0.344	26.2
6.56	0.256	25.0
11.25	0.216	27.5
16.58	0.213	26.3
19.69	0.192	27.5

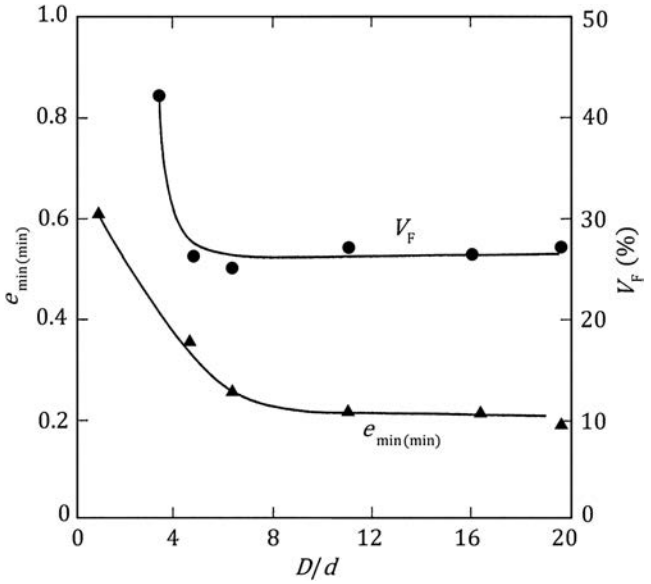

Figure 1.42 Test results of McGeary (1961)—Variation of $e_{min(min)}$ and V_F with D/d.

Table 1.8 $D_{50\text{-sand}}$ and $D_{50\text{-fines}}$ of the soils used by Lade et al. (1998)

Sand description	$D_{50\text{-sand}}$ *(mm)*	$D_{50\text{-fines}}$ *(mm)*	$\frac{D_{50\text{-sand}}}{D_{50\text{-fines}}}$
Nevada 50/80	0.211	0.050	4.22
Nevada 80/200	0.120	0.050	2.4

- For a given sand and fine mixture, the e_{max} and e_{min} decrease with the increase in the volume of fines from zero to about 30%. This is approximately similar to the behavior of ideal spheres shown in Figures 1.41 and 1.42. This is the *filling-of-the-void phase* where fines tend to fill the void spaces between the larger sand particles.
- There is a *transition zone*, where the percentage of fines is between 30 and 40%.
- For percentage of fines greater than about 40%, the magnitudes of e_{max} and e_{min} start increasing. This is the *replacement-of-solids phase*, where larger-sized solid particles are pushed out and gradually replaced by fines.

1.15 SOIL CLASSIFICATION SYSTEMS

Soil classification is the arrangement of soils into various groups or subgroups to provide a common language to express briefly the general usage characteristics

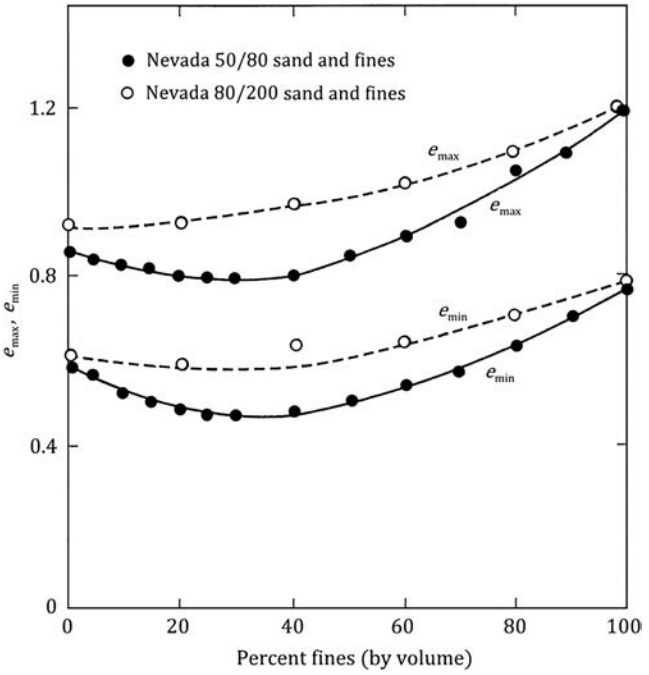

Figure 1.43 Variation of e_{max} and e_{min} with percent of nonplastic fines (Based on the test results of Lade et al., 1998). *Note*: For 50/80 sand and fines, $D_{50\text{-sand}}/D_{50\text{-fines}}$ = 4.22 and, for 80/200 sand and fines, $D_{50\text{-sand}}/D_{50\text{-fines}}$ = 2.4.

without detailed descriptions. At the present time, two major soil classification systems are available for general engineering use. They are the unified system and the American Association of State Highway and Transportation Officials (AASHTO) system. Both systems use simple index properties such as grain-size distribution, liquid limit, and plasticity index of soil.

1.15.1 Unified system

The unified system of soil classification was originally proposed by A. Casagrande in 1948 and was then revised in 1952 by the Corps of Engineers and the U.S. Bureau of Reclamation. In its present form [also see ASTM D-2487, ASTM (2014)], the system is widely used by various organizations, geotechnical engineers in private consulting business, and building codes.

Initially, there are two major divisions in this system. A soil is classified as a coarse-grained soil (gravelly and sandy) if more than 50% is retained on a No. 200 sieve and as a fine-grained soil (silty and clayey) if 50% or more is passing through a No. 200 sieve. The soil is then further classified by a number of subdivisions, as shown in Table 1.9.

Table 1.9 Unified soil classification system

Major divisions	*Group symbols*	*Typical names*	*Criteria or classification*[a]
Coarse-grained soils (<50% passing No. 200 sieve)[a]			
Gravels (<50% of coarse fraction passing No. 4 sieve)			
Gravels with few or no fines	GW	Well-graded gravels; gravel–sand mixtures (few or no fines)	$C_u = \frac{D_{60}}{D_{10}} > 4; \quad C_c = \frac{(D_{30})^2}{(D_{10})(D_{60})}$ Between 1 and 3
	GP	Poorly graded gravels; gravel–sand mixtures (few or no fines)	Not meeting the two criteria for GW
Gravels with fines	GM	Silty gravels; gravel–sand–silt mixtures	Atterberg limits below *A*-line *or* plasticity index less than 4[b] (see Figure 1.44)
	GC	Clayey gravels; gravel–sand–clay mixtures	Atterberg limits above *A*-line *with* plasticity index greater than 7[b] (see Figure 1.44)
Sands (≥50% of coarse fraction passing No. 4 sieve)			
Clean sands (few or no fines)	SW	Well-graded sands; gravelly sands (few or no fines)	$C_u = \frac{D_{60}}{D_{10}} > 6; \quad C_c = \frac{(D_{30})^2}{(D_{10})(D_{60})}$ Between 1 and 3
	SP	Poorly graded sands; gravelly sands (few or no fines)	Not meeting the two criteria for SW

Sands with fines (appreciable amount of fines)	SM	Silty sands; sand–silt mixtures	Atterberg limits below *A*-line *or* plasticity index less than 4[b] (see Figure 1.44)
	SC	Clayey sands; sand–clay mixtures	Atterberg limits above *A*-line *with* plasticity index greater than 7[b] (see Figure 1.44)
Fine-grained soils (≥50% passing No. 200 sieve)			
Silts and clay (liquid limit less than 50)	ML	Inorganic silts; very fine sands; rock flour; silty or clayey fine sands	See Figure 1.44
	CL	Inorganic clays (low to medium plasticity); gravelly clays; sandy clays; silty clays; lean clays	See Figure 1.44
	OL	Organic silts; organic silty clays (low plasticity)	See Figure 1.44
Silts and clay (liquid limit greater than 50)	MH	Inorganic silts; micaceous or diatomaceous fine sandy or silty soils; elastic silt	See Figure 1.44
	CH	Inorganic clays (high plasticity); fat clays	See Figure 1.44
	OH	Organic clays (medium to high plasticity); organic silts	See Figure 1.44
Highly organic silts	Pt	Peat; mulch; and other highly organic soils	

Group symbols are G, gravel; W, well-graded; S, sand; P, poorly graded; C, clay; H, high plasticity; M, silt; L, low plasticity; O, organic silt or clay; Pt, peat and highly organic soil.

[a] Classification based on percentage of fines: <5% passing No. 200: GW. GP. SW. SP: >12% passing No. 200: GM. GC. SM. SC: 5%–12% passing No. 200: borderline—dual symbols required such as GW–GM. GW–GC. GP–GM. GP–SC. SW–SM. SW–SC. SP–SM. SP–SC.

[b] Atterberg limits above *A*-line and plasticity index between 4 and 7 are borderline cases. It needs dual symbols (see Figure 1.44).